ARTICLE TEMPLATE

Pareto optimal synthesis of eight-bar mechanism using meta-heuristic multi-objective search approaches: Application to bipedal gait generation

Miguel Gabriel Villarreal-Cervantes[a], Jesús Said Pantoja-García[b], Alejandro Rodríguez-Molina[c] and Saul Enrique Benitez-Garcia[a]

[a]Posgraduate Department, Instituto Politécnico Nacional, CIDETEC, Mexico city, 07700, Mexico.
[b]Universidad Tecnológica de México – UNITEC MÉXICO – Campus Atizapán, Estado de México, 52999, Mexico.
[c]Tecnológico Nacional de México / IT de Tlalnepantla, Research and Postgraduate Division, Estado de México, 54070, México.

ARTICLE HISTORY
Compiled June 11, 2021

ABSTRACT
The structural complexity of the bipedal locomotion may be reduced by using mechanisms with fewer actuators, which ideally do not degrade the performance and functionality of the robot. However, when the mechanism design considers conflicting design objectives, the search for design solutions with specific trade-offs becomes hard. This work studies different multi-objective search approaches the dominance-based, the decomposition-based, and the metric-driven in the dimensional synthesis of the eight-bar mechanism for the bipedal locomotion application in the sagittal plane stated as a mixed discrete-continuous nonlinear multi-objective optimization problem. Also, this work proposes a dominance-based multi-objective differential evolution algorithm called Multi-Objective Specialist Population-based Differential Evolution (MOSPDE), which endows specialized subpopulations to exploit different regions of the Pareto front to favor the search for design trade-offs with a suitable generation of the gait and force transmission during the stance phase. The comparative study includes algorithms reported in the specialized literature based on dominance (MOPSO, MODE variants, and NSGA-II), decomposition (MOEA/D-DE), and metric-driven (SMS-EMOA). The statistical analysis reveals that using the Pareto dominance search approach based on differential evolution and the inclusion of exhaustive exploitation can promote the reconfigurability of the bipedal locomotion mechanism with better trade-offs that satisfy the conflicting design objectives.

KEYWORDS
Optimal synthesis; gait generation; multi-objective optimization; meta-heuristic algorithms

CONTACT Miguel Gabriel Villarreal-Cervantes Email: mvillarrealc@ipn.mx

1. Introduction

The bipedal locomotion study in robotic systems has increased in the last years due to it can aid the design of exoskeletons (Aliman, Ramli, & Haris, 2017), robotic prostheses (Richter, Simon, Smith, & Samorezov, 2015), service robots, among others. In this context, the bipedal gait is a complex task that requires a human movement analysis to be optimized (Lim, Kwon, & Park, 2014). It generally needs a robotic system with twelve degrees of freedom ($d.o.f.$) to suitably perform such a trajectory, and a complex control system to move smoothly. Control strategies applied so far to bipedal walking are related to the zero moment point (ZMP) principle (Vukobratovic & Borovac, 2004), advanced control schemes (Arcos-Legarda, Cortes-Romero, & Tovar, 2019), and the use of intelligent techniques such as fuzzy logic (Yang, Liu, & Chen, 2019), and neuronal networks for instance in Central Pattern Generators that produce rhythmic output patterns in the control of robotic legged locomotion (Garcia-Saura, 2015), (Matos & Santos, 2014), (Pinto & Golubitsky, 2006). Nevertheless, there is another design approach that does not take into account the human model but the design of a specific function (Yoneda, Tamaki, Ota, & Kurazume, 2003). Through time, researchers have reduced the biped walking complexity by decreasing actuators (Ito et al., 2018), using springs in unactuated joints (Alexander, 1990), proposing flexible links (Sarkar & Dutta, 2015), or even mechanisms in the knee (Aoustin & Hamon, 2013) and limbs (Gui, 2019). Low $d.o.f.$ mechanisms (Uicker, Pennock, & Shigley, 2010) for biped robots would be essential for specific tasks since they decrease the energy consumption due to the reduction of the robot weight and the number of actuators. Also, they can perform the same trajectory in its linkages by the rotation of the crank link (actuated joints) by using or not simple velocity controllers (Kajita, Hirukawa, Harada, & Yokoi, 2014). So, the dimensional synthesis of mechanisms can be optimized to guarantee the tracking of different desired precision points (for example related to the biped gait). Generally, biped gait movements are notoriously difficult to be reproduced by robots. Several current works have proposed different alternatives to replicate the gait movement in legged robots, among them are the Watt's six-bar mechanism (Mehdigholi & Akbarnejad, 2012) and the six-bar Stephenson linkage (Tsuge, Plecnik, & McCarthy, 2016). Other options for lower limb rehabilitation include the use of a six-bar mechanism (Wang, Yu, Chou, & Chang, 2009) and a cam-seven-bar crank-slider mechanism (Shao, Xiang, Liu, & Li, 2016). In recent years, much attention has been paid to form eight-bar systems by coupling different mechanisms for limb movements (Gui, 2019) (also see references cited therein) because they can provide considerable flexibility in the synthesis (Waldron, Kinzel, & Agrawal, 2016) which can result in better quality in the design objectives.

A single $d.o.f.$ mechanism can trace complex planar curves like the ankle trajectory in the gait. Nevertheless, traditional synthesis methods (Sandor & Erdman, 1984) are not suitable for closed trajectories due to the increment of precision points, resulting in an overdetermined system of equations that describe the mechanism behavior and whose exact solution can not be obtained. So, mechanism synthesis has been formulated as optimization problems where efficient optimization techniques must be used. Gradient-based algorithms (Chanekar, Fenelon, & Ghosal, 2013) and meta-heuristic algorithms (Bulatović, Dordević, & Dordević, 2013; Bulatović, Miodragović, & Bošković, 2016; Ebrahimi & Payvandy, 2015; Lin, 2010; Ortiz, Cabrera, Nadal, & Nadal, 2013; Sleesongsom & Bureerat, 2017) have been used as optimization techniques to guide the search for optimal link lengths. However, meta-heuristic algorithms

(MHAs) (Coello, Lamont, & Veldhuizen, 2007) are gaining more attention than the gradient ones (Bazaraa, Sherali, & Shetty, 2006), because the latter converge to a solution near the initial one, get stuck in suboptimal solutions, and are dependent of the problem characteristic (discontinuous, nonlinear, discrete, etc.). In contrast, MHAs converge to a most promising region no matter the problem characteristics (robustness), their implementation is simple, and they are derivative-free algorithms whose performance may be improved by endowing them with mixed features of other MHAs.

The performance of the path generation in the biped gait mechanism also depends on other design objectives considered in the multi-objective optimization problem such as the maximum torque, the energy transfer in the stance phase, the dexterity, the static efficiency, the stiffness in the gait, etc. Such objectives are usually in "conflict," i.e., the problem does not have a single minimum solution. So, a set of solutions (called non-dominated solutions) with different design trade-offs are obtained. This set provides the designer with several mechanism reconfigurations (Pareto front solutions) to make the decision making (Russo, Herrero, Altuzarra, & Ceccarelli, 2018).

The optimal mechanism design that takes into account different conflicting requirements has been an essential issue in the last decade. Two main methods have been proposed in the literature to handle multi-objective optimization problems: The first one is the scalarization method (Osycska, 1984) where the multi-objective optimization problem is transformed into a single-objective optimization one (Ebrahimi & Payvandy, 2015; Sancibrian, Sarabia, Sedano, & Blanco, 2016; Ávila Hernández & Cuenca-Jiménez, 2018). This method includes approaches like weighted sums, goal programming, ε-constraint, among others. The main drawback is the high sensitivity of weights to the design criteria such that an evenly distributed set of weights does not necessarily produce an evenly distributed representation of the Pareto-optimal set (trade-offs), i.e., different weights may produce nearly similar design vectors. Then, a trial-and-error procedure in the selection of weights is commonly used to find diverse non-dominated solutions (Pareto-optimal solutions), and only a limited set of solutions can be found (one per optimization process with a predefined weight selection). Moreover, particular desired trade-offs are difficult to fulfill since the weight space and the Pareto front space present a nonlinear relationship. When more than one performance functions are considered in the mechanism synthesis, the majority of the reviewed works transform the multi-objective optimization problem into a mono-objective optimization one (by a scalarization method). Also, meta-heuristic algorithms (MHAs) are frequently used to solve the problem. According to (Sleesongsom & Bureerat, 2017), the most used MHAs in the mechanism optimal design stated as a mono-objective optimization problem, are differential evolution (DE), follow by Genetic Algorithms (GAs), the Particle Swarm Optimization (PSO) and the Imperialist Competitive Algorithm (ICA).

On the other hand, the second method refers to the use of multi-objective optimization (Coello et al., 2007), where multiple optimal solutions are found in one single run considering three main goals: *i*) to converge to the true Pareto front $\mathcal{PF}^*$, even when in real-world optimization problems this front is not known and then, the convergence is to the best Pareto front approximation $\mathcal{PF}^A$; *ii*) to find widely and uniformly spread solutions (diversity); *iii*) to maintain multiple non-dominated solutions. Hence, multi-objective optimization aims the simultaneous optimization of different performance requirements and has been applied in mechatronic design (Portilla-Flores et al., 2011), (Villarreal-Cervantes, 2017), in control tuning (Villarreal-Cervantes, Rodríguez-

Molina, García-Mendoza, Peñaloza-Mejía, & Sepúlveda-Cervantes, 2017), (Reynoso-Meza, Blasco, Sanchis, & Martínez, 2014) and more scarcely in mechanism (Cabrera, Nadal, Muñoz, & Simon, 2007; EL-Kribi, Houidi, Affi, & Romdhane, 2013; Khorshidi, Soheilypour, Peyro, Atai, & Panahi, 2011; Nariman-Zadeh, Felezi, Jamali, & Ganji, 2009).

The study of search approaches in the mechanism design with different requirements can improve the trade-offs in the bipedal gait generation through "simple" mechanisms. The literature of the studies about dimensional synthesis through multi-objective optimization (second method) is reviewed next; to the best of the author's knowledge, few works address such a problem. In (Cabrera et al., 2007), the design of a hand robot mechanism is formulated as a multi-objective optimization problem considering five performance functions related to the tracking error, the grasping index, the acceleration in the contact point, the weight of the mechanism, and the standardization of the mechanism link lengths. The Pareto optimum evolutionary multi-objective algorithm is used to solve the problem. This algorithm finds several solutions from which the designer can posteriorly choose the best one for the particular application. Moreover, the implementation simplicity of the algorithm allows it to be used in other synthesis problems. The multi-objective hybrid genetic algorithm is used in (Nariman-Zadeh et al., 2009) to design a four-bar mechanism with efficient trade-offs between the tracking error and transmission angle error. Simulation results reveal that superior mechanisms are obtained when compared with those reported in the literature. The design of a four-bar mechanism that considers the tracking error, the deviation of the transmission angles, and the maximum angular velocity ratio, is presented in (Khorshidi et al., 2011). The Pareto Genetic Algorithm with Adaptive Local Search is proposed to improve the obtained solutions by performing a refined local search into the neighborhood of promising non-dominated points. The concurrent design of a four-bar mechanism driven by a DC motor is detailed in (EL-Kribi et al., 2013), where the mechanical load and the voltage fluctuation are used as the performance functions to be optimized. The corresponding multi-objective optimization problem with continuous and discrete variables is stated and then solved by the Non-dominated Sorting Genetic Algorithm II (NSGA-II). The continuous parameters are related to the kinematic and dynamic parameters of the four-bar mechanism; meanwhile, the discrete ones are related to the motor selection. The NSGA-II can obtain a better redistribution of the mechanical system dynamic parameters and also a better choice of the driving motor.

From the literature review, few research works handle the multiple objectives as multi-objective optimization problems (second method). In these researches, MHAs based on Pareto dominance are included to search into the design space for finding the best quality Pareto front approximation (dominance-based search). Other search approaches like the decomposition-based, where the multi-objective optimization problem is decomposed into scalar optimization sub-problems and optimized simultaneously; or metric-driven, where a specific performance metric is used to guide the search, have not been yet studied in the dimensional synthesis of mechanisms. As established in the "No Free Lunch" and "Free Leftover" theorems (Corne & Knowles, 2003), it is necessary to compare different algorithms (different search approaches) to select a set of promising alternatives, and also, to provide evidence of the most useful search approaches in the dimensional synthesis of mechanisms. Hence, to the best of the author's knowledge, there is a gap in the comparative study of different search approaches (dominance-based, decomposition-based and metric-driven) which can help to find a Pareto front with better diversity, convergence, and more design trade-offs

in the dimensional synthesis of the eight-bar mechanism for bipedal gait. This can aid researchers interested in applying multi-objective optimization algorithms in the kinematic synthesis of this kind of problem, by providing them with some insights about the advantages or limitations of the studied multi-objective search approaches, and also some observations on how the search is performed with the most promising algorithms. So, the researchers can have some basic guidelines for selecting an initial set of algorithms to make the optimum kinematic synthesis.

Therefore, this work presents a comparative study of the three most representative and recent multi-objective search approaches in MHAs for the mechanism synthesis. Five MHAs are based on Pareto dominance: the Multi-Objective Differential Evolution (MODE) (Price, Storn, & Lampinen, 2005), the Multi-Objective Differential Evolution with reconfigurability promotion by a crowding mechanism (CR-MODE) (Portilla-Flores et al., 2011), the Multi-Objective Exhaustive Exploitation Differential Evolution(MOEEDE) (Villarreal-Cervantes, 2017), the Non-dominated Sorting Genetic Algorithm II (NSGAII) (Deb, Pratap, Agarwal, & Meyarivan, 2002), and the Multiple Objective Particle Swarm Optimization (MOPSO) (Coello, Pulido, & Lechuga, 2004). One MHA is based on decomposition: the Multi-objective Evolutionary Algorithm based on Decomposition and Differential Evolution (MOEA-D) (Zhang & Li, 2007). The last MHA is based on a metric-driven search: S-Metric Selection Evolutionary Multi-objective Algorithm (SMS-EMOA) (Beume, Naujoks, & Emmerich, 2007). A particular case study "the synthesis of an eight-bar mechanism" for the bipedal locomotion in the sagittal plane is proposed to be solved by three different multi-objective search approaches included in the seven MHAs. The selection of the eight-bar mechanism is that it has high flexibility (design reconfigurability) in synthesis, compared with other mechanisms with fewer linkages, such as the four-bar mechanism (the most common mechanism reported in the literature) (Waldron et al., 2016). So, this can be useful in the obtained design trade-offs which will impact the application.

Besides, a dominance-based algorithm called Multi-Objective Specialist Population-based Differential Evolution algorithm (MOSPDE) is also proposed and compared to the other alternatives. The results reveal that the dominance-based search approach with the inclusion of exploitation of different Pareto regions promotes the search for fronts with better convergence, diversity and a higher number of non-dominated solutions. As the MHAs are stochastic techniques, their performance is confirmed and compared by using non-parametric statistical tests (Derrac, García, Molina, & Herrera, 2011) to draw valid conclusions.

The rest of the paper is organized as follows: The optimization problem related to the study case of eight-bar mechanism synthesis for the bipedal gait generation is described in Section 2. In Section 3, the multi-objective optimization concepts and the different search approaches are reviewed; then, the proposed optimization strategy is described. The comparative results of six optimizers based on Pareto dominance, one based on decomposition, and one based on the metric-driven approach, are analyzed and discussed in Section 4. Finally, the conclusions are drawn in Section 5.

2. Study case: Optimal design for a lower-limb mechanism

The one degree of freedom eight-bar mechanism (Pantoja-García, Villarreal-Cervantes, González-Robles, & Cervantes, 2017) shown in Fig. 1 is selected as the lower limb

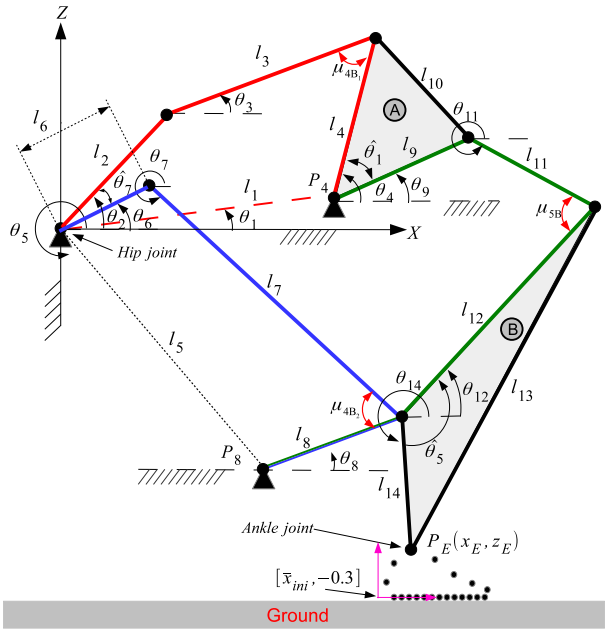

Figure 1.: Bipedal lower-limb mechanism.

of biped robots for walking in the sagittal plane with the Cartesian coordinate $P_E = [x_E, z_E]$. The associated parameters in the figure are: the link length vector $\vec{l} = (l_1, l_2, \ldots, l_{14})$, the link angular displacements $\vec{\theta} = (\theta_1, \theta_2, \ldots, \theta_{14})$, and the interior angles of the triangular links $\hat{\theta}_1, \hat{\theta}_5$.

In this paper, the optimal design of such mechanism is considered as a study case for applying the meta-heuristic multi-objective search approaches. The design variables of the eight-bar mechanism are the link lengths $l_i \quad \forall\ i = 1, 2, ..., 9, 11, 12, 14$, the angles θ_1, θ_5 of the fixed links, the interior angles $\hat{\theta}_1, \hat{\theta}_5$ of the triangular links, the angle deviation $\hat{\theta}_7$, the position $[\bar{x}_{ini}, -0.3]$ of the gait trajectory coordinate system , the kinematic configurations of the sub-mechanisms $m_b = \{m_{4b_1}, m_{4b_2}, m_{5b}\}$ (elbow-up and elbow-down configuration (Pantoja-García et al., 2017)), and the $\bar{n}$ angular displacements of the crank $\theta_2 = \{\theta_2^i \mid i = 1, 2, \ldots, \bar{n}\}$. Those variables are grouped in the vector $\vec{x} = [l_i, \theta_1, \theta_5, \hat{\theta}_1, \hat{\theta}_5, \hat{\theta}_7, \bar{x}_{ini}, m_b, \theta_2]^T \in R^{21+\bar{n}}$, which includes both continuous and discrete variables. Discrete variables m_b are included into the kinematic configuration vector which can have two different discrete values -1 or 1.

The kinematics of the eight-bar mechanism, grouped by the expression $\Theta = f(\vec{x})$, is obtained in (Pantoja-García et al., 2017) by assuming three sub-mechanisms (two four-bar and one five-bar mechanism) and those are presented in (1) and (2).

$$\theta_{j+k} = 2atan2\left(-\hat{B} + m_{4b_\alpha}\,(-1)^{\beta}\sqrt{\hat{B}^2 + \hat{A}^2 - \hat{C}^2}, \hat{C} - \hat{A}\right)$$
$$\forall j = 0, 4 \wedge k = 3, 4 \tag{1}$$
$$\theta_{o+11} = 2atan2\left(-\bar{B} + m_{5b}(-1)^{o}\sqrt{\bar{B}^2 + \bar{A}^2 - \bar{C}^2}, \bar{C} - \bar{A}\right)$$
$$\forall o = 0, 1 \tag{2}$$

where:

$$\alpha = \frac{(j-2)^j}{\left(\sqrt[4]{j+4}\right)^j}$$

$$\beta = (j+k+1)$$

$$\hat{A} = (-1)^k 2 l_{j+1} l_{j+k} \cos(\theta_{j+1}) + (-1)^{k+1} 2 l_{j+2} l_{j+k} \cos(\theta_2)$$

$$\hat{B} = (-1)^k 2 l_{j+1} l_{j+k} \sin(\theta_{j+1}) + (-1)^{k+1} 2 l_{j+2} l_{j+k} \sin(\theta_2)$$

$$\begin{aligned}\hat{C} = {} & l_{j+1}^2 + l_{j+2}^2 + (-1)^{k+1} l_{j+3}^2 + (-1)^k l_{j+4}^2 \\ & -2 l_{j+1} l_{j+2} \cos(\theta_{j+1} - \theta_2)\end{aligned}$$

$$\begin{aligned}\bar{A} = {} & (-1)^{o+1} 2 l_{o+11} l_{8(1-o)+15o} \cos\theta_{8(1-o)+15o} \\ & +(-1)^o 2 l_9 l_{o+11} \cos\theta_9 \\ & +(-1)^{o+1} 2 l_{o+11} l_{8o+15(1-o)} \cos\theta_{8o+15(1-o)}\end{aligned}$$

$$\begin{aligned}\bar{B} = {} & (-1)^{o+1} 2 l_{o+11} l_{8(1-o)+15o} \sin\theta_{8(1-o)+15o} \\ & +(-1)^o 2 l_9 l_{o+11} \sin\theta_9 \\ & +(-1)^{o+1} 2 l_{o+11} l_{8o+15(1-o)} \sin\theta_{8o+15(1-o)}\end{aligned}$$

$$\begin{aligned}\bar{C} = {} & l_8^2 + l_9^2 + l_{o+11}^2 + l_{15}^2 - l_{12-o}^2 \\ & +(-1)^{o+1} 2 l_8 l_{9(1-o)+15o} \cos\left(\theta_8 - \theta_{9(1-o)+15o}\right) \\ & +(-1)^o 2 l_8 l_{9o+15(1-o)} \cos\left(\theta_8 - \theta_{9o+15(1-o)}\right) \\ & -2 l_9 l_{15} \cos\left(\theta_9 - \theta_{15}\right)\end{aligned}$$

The mechanism design, stated as a nonlinear multi-objective optimization problem, consists on finding the design variable vector $\vec{x}$ that optimizes the conflictive objective functions related to the accuracy in the generation of the human gait path f_1 on the sagittal plane, and the force transmission f_2 during the stance phase from the input link l_2 to the output point PE, subject to the inequality constraints due to the Grashof criterion in (4)-(9), the functional morphology in (10)-(12), the movement validation (13)-(14); the equality constraints due to the kinematic behavior in (15), the desired gait $\bar{P}_E = [\bar{x}_E, \bar{z}_E]$ in (16)-(17); and the bounds of the design variables (18). Consult (Pantoja-García et al., 2017) for more details about the equations related to the optimization problem formulation. It is important to point out that finding the solution to this optimization problem is a hard task due to the inclusion of mixed continuous-discrete design variables.

$$\min\left[f_1\left(\vec{x}\right), f_2\left(\vec{x}\right)\right] \tag{3}$$

Table 1.: Bounds of the design variables.

Bounds	l_i	θ_1	θ_5	$\hat{\theta}_1$	$\hat{\theta}_5$	$\hat{\theta}_7$	$\bar{x}_s$	m_b	θ_2
$\vec{x}_l$	0	0	0	0	0	0	$-\frac{1}{2}$	-1	0
$\vec{x}_u$	0.2	2π	2π	π	π	2π	$\frac{1}{2}$	1	2π

subject to:

$$g_1 : l_2 + l_1 - l_3 - l_4 < 0 \tag{4}$$
$$g_2 : l_6 + l_5 - l_7 - l_8 < 0 \tag{5}$$
$$g_3 : -l_4 - l_1 + l_2 + l_3 < 0 \tag{6}$$
$$g_4 : -l_3 - l_1 + l_2 + l_4 < 0 \tag{7}$$
$$g_5 : -l_8 - l_5 + l_6 + l_7 < 0 \tag{8}$$
$$g_6 : -l_7 - l_5 + l_6 + l_8 < 0 \tag{9}$$
$$g_7 : -P_{11y} - 0.25 < 0 \tag{10}$$
$$g_8 : -P_{8y} - 0.25 < 0 \tag{11}$$
$$g_9 : -P_{4y} - 0.25 < 0 \tag{12}$$
$$g_{9+i} : \hat{B}^2 + \hat{A}^2 - \hat{C}^2 \geq 0 \ \forall \ i = 1, ..., \bar{n} \tag{13}$$
$$g_{9+\bar{n}+j} : \bar{B}^2 + \bar{A}^2 - \bar{C}^2 \geq 0 \ \forall \ j = 1, ..., \bar{n} \tag{14}$$
$$h_1 : \Theta - f(\vec{x}) = 0 \tag{15}$$
$$h_2 : \bar{x}_E - \left(\tilde{l}_1 \sin\tilde{\theta}_1 + \tilde{l}_2 \sin\left(\tilde{\theta}_1 - \tilde{\theta}_2\right) 0\right) f_x - \bar{x}_{ini} = 0 \tag{16}$$
$$h_3 : \bar{z}_E - \left(\tilde{l}_1 \cos\breve{\theta}_1 + \tilde{l}_2 \cos\left(\breve{\theta}_1 - \breve{\theta}_2\right) - \tilde{l}_1 \cos\tilde{\theta}_1 - \tilde{l}_2 \cos\left(\tilde{\theta}_1 - \tilde{\theta}_2\right)\right) f_z + 0.3 = 0 \tag{17}$$
$$\vec{x}_l \leq \vec{x} \leq \vec{x}_u \tag{18}$$

The upper and lower bounds are given in Table 1 and the coordinates P_y of mechanism joints are set as $P_{4y} = l_1 \sin(\theta_1)$, $P_{8y} = l_5 \sin(\theta_5)$, $P_{11y} = l_6 \sin(\theta_6) + l_7 \sin(\theta_7) + l_{12} \sin\theta_{12}$.

Unlike the mono-objective optimization problem stated in (Pantoja-García et al., 2017), a multi-objective optimization problem formulation is stated in this work. In this problem, the first design objective f_1, displayed in (19), is related to the accuracy to reach the $\bar{n}$ precision points of the desired path $\bar{P}_E = [x_E, \bar{z}_E]$ by the point P_E of the gait mechanism; the second criterion f_2, shown in (20), provides a design with the most suitable force transmission during the stance phase of the gait mechanism. This last criterion is related to the deviation of the transmission angle of three sub-mechanisms $\mu_\varrho \mid \varrho = \{4B_1, 4B_2, 5B\}$ from the ideal one (pressure angle (Balli & Chand, 2002)). The transmission angle related to the four-bar mechanism is obtained by considering the maximum and minimum angular displacement in $\mu_\varrho \mid \varrho = \{4B_1, 4B_2\}$, while the one related to the five-bar mechanism is obtained in the stance phase. Also, the other difference is the inclusion of the discrete variables related to the elbow-up and elbow-down four-bar mechanism configurations which promotes more reconfigurability of the lower limb design.

Table 2.: Hip angles ($\tilde{\theta_1}$) and knee angles ($\tilde{\theta_2}$) obtained from (Bovi et al., 2011).

$\bar{n}$	$\tilde{\theta_1}$	$\tilde{\theta_2}$	$\breve{\theta_1}$	$\breve{\theta_2}$	$\bar{n}$	$\tilde{\theta_1}$	$\tilde{\theta_2}$	$\breve{\theta_1}$	$\breve{\theta_2}$
1	27.9	8.8	27.9	8.8	11	−7	9.7	−7	9.7
2	27.6	12.9	27.6	12.9	12	−10.2	11.1	−10.2	11.1
3	26.6	19	26.6	19	13	−12.5	14.4	−12.5	14.4
4	23.9	22.1	23.9	22.1	14	−11.8	29	27.3	16.1
5	19.8	21.6	19.8	21.6	15	−1.9	50.8	23	22.2
6	15.1	19.3	15.1	19.3	16	12.2	65.3	15.1	19.3
7	10.3	16.5	10.3	16.5	17	23.4	61.9	6.7	14.6
8	5.5	13.9	5.5	13.9	18	29.4	44.4	−1.3	10.7
9	0.9	11.6	0.9	11.6	19	29.5	19.2	−7.9	9.9
10	−3.3	10	−3.3	10	20	27.5	5.5	−12.5	14.4

$$f_1 = \sum_{i=1}^{\bar{n}} \left(\bar{x}_E^i - x_E^i\right)^2 + \sum_{i=1}^{\bar{n}} \left(\bar{z}_E^i - z_E^i\right)^2 \tag{19}$$

$$f_2 = \sum_{k=1}^{2} \left(\mu_{4B_1} - \frac{\pi}{2}\right)^2 + \sum_{k=1}^{2} \left(\mu_{4B_2} - \frac{\pi}{2}\right)^2 + \sum_{j=12}^{\bar{n}} \left(\mu_{5B} - \frac{\pi}{2}\right)^2 \tag{20}$$

where:

$x_E^i = l_6 \cos\theta_2^i + l_7 \cos\theta_7^i + l_{14} \cos\theta_{14}^i$

$z_E^i = l_6 \sin\theta_2^i + l_7 \sin\theta_7^i + l_{14} \sin\theta_{14}^i$

$\mu_{4B_1} = \cos^{-1}\left(\frac{l_3^2 + l_4^2 - (l_1 - l_2(-1)^k)^2}{2 l_3 l_4}\right)$

$\mu_{4B_2} = \cos^{-1}\left(\frac{l_7^2 + l_8^2 - (l_5 - l_6(-1)^k)^2}{2 l_7 l_8}\right)$

$\mu_{5B} = \theta_{12}^j - \theta_{11}^j + 2\pi$

Another difference concerning the optimization formulation in (Pantoja-García et al., 2017) is related to the desired trajectory where a semicircular trajectory is chosen. In the present work, the desired path is parameterized by considering the hip-knee angles and the lengths $\tilde{l}_1 = 0.416m$, $\tilde{l}_2 = 0.418m$, presented in the biomechanical study in (Bovi, Rabuffetti, Mazzoleni, & Ferrarin, 2011), to provide a more realistic gait behavior. Twenty hip-knee angles of a group of people between 6 to 12 years old collected from such study are used and shown in Table 2. As a result, the number precision points for the desired path is $\bar{n} = \bar{n}_a + \bar{n}_b = 20$, where $\bar{n}_a = 13$ means that 65% of the gait cycle is in the stance phase, and $\bar{n}_b = 7$ means that 35% of the gait cycle is in the swing phase. This path is resized to a small-scale for using it in the design of small biped legs and is presented in (16) and (17), where the scale factor $f_x = 0.0001125$, $f_z = 0.00025$ yields a small-scaled gait trajectory with a step length of about $0.08m$, and a step elevation of about $0.04m$.

3. Optimization strategy

In mechanism synthesis, different solutions can provide distinct trade-offs between the performance functions. The importance of using an appropriate optimizer in an optimal design (Villarreal-Cervantes, 2017) is a crucial task to find the most suitable trade-off for the application, which provides a synergy between performance functions. The optimization algorithm must be able to explore the search space efficiently. Also, it must highly promote the exploitation of the most promising solutions to contribute a widespread Pareto front and to approximate it to the true Pareto front, even when such front is not generally known in engineering applications. Hence, in this paper, subpopulations are incorporated into the multi-objective differential evolution algorithm, which independently explores different areas of the search space in a different way to promote the exploration of different regions of the Pareto front. Moreover, a simple intercommunication, but efficient procedure among subpopulations, is proposed to introduce a superior subpopulation that stores the best trade-offs of the optimization problem.

3.1. Fundamentals of multi-objective optimization

The fundamental concepts of multi-objective optimization are detailed below (Coello et al., 2007).

Definition 1. *Feasible region: Let $\bar{p} \in \Omega$ be all design space solutions. The feasible region is represented as $\hat{\Omega} = \{\bar{p} \in \Omega \mid g(\bar{p}) < 0, h(\bar{p}) = 0\}$*

Definition 2. *Domination: A vector $\varrho = [\varrho_1, ..., \varrho_k]^T$ dominates a vector $\nu = [\nu_1, ..., \nu_k]^T$ (denoted as $\varrho \preceq \nu$), if and only if, ϱ is smaller than ν, i. e., $\forall i \in \{1, ..., k\}$, $\varrho_i \leq \nu_i \wedge \exists i \in \{1, ..., k\} : \varrho_i < \nu_i$.*

Definition 3. *Pareto optimality: A solution $\bar{p} \in \hat{\Omega}$ is a Pareto optimum in $\hat{\Omega}$, if and only if, there is no $\bar{p}' \in \hat{\Omega}$ for which $\nu = J(\bar{p}') = [J_1(\bar{p}'), ..., J_i(\bar{p}')]^T$ dominates $\varrho = J(\bar{p}) = [J_1(\bar{p}), ..., J_i(\bar{p})]^T$.*

Definition 4. *Pareto optimal set: It is defined as $\mathfrak{P}^* := \{\bar{p} \in \hat{\Omega} \mid \nexists\ \bar{p}' \in \hat{\Omega}\ ,\ J(\bar{p}') \preceq J(\bar{p})\}$*

Each solution $\bar{p} \in \mathfrak{P}^*$ is called non-dominated solution.

Definition 5. *Pareto front: It is defined as $\mathfrak{PF} := \{u = J(\bar{p}) \mid \bar{p} \in \mathfrak{P}^*\}$*

3.2. Multi-objective specialist population based differential evolution algorithm

In the last decade, the Differential Evolution (DE) algorithm (Price et al., 2005), has been one of the most used and efficient evolutionary algorithms for numerical optimization because of its success in academic benchmark competitions and also in real engineering applications. The proposed multi-objective specialist population-based differential evolution algorithm (MOSPDE) solves the constrained multi-objective opti-

mization problem in the dimensional synthesis presented in Section 2. The MOSPDE promotes finding Pareto fronts with spread and diversity to provide to the designer with a broad set of mechanism design solutions with different trade-offs. In this section, the proposal is explained.

In the first part of the algorithm, three parent subpopulations with NP individuals are randomly generated in the interval $[\vec{x}^i_{j,G_\varphi,MIN}, \vec{x}^i_{j,G_\varphi,MAX}]$ and stored in $\mathbf{X}_{G_\varphi} = [\vec{x}^1_{G_\varphi}, ..., \vec{x}^{NP}_{G_\varphi}]^T \in R^{NP\times D}\ \forall\ \varphi = 1, ..., 3 \wedge G = 1$, where φ is referred to the index of the subpopulation and G is the generation number. Each individual $\vec{x}^i_{G_\varphi} = [\vec{x}^i_{1,G_\varphi}, ..., \vec{x}^i_{D,G_\varphi}]^T \in R^{1\times D}$ is a potential design variable vector $\bar{p} \in R^D$ in the optimization problem, where $\vec{x}^i_{j,G_\varphi,MIN} = \bar{p}_{MIN}$ and $\vec{x}^i_{j,G_\varphi,MAX} = \bar{p}_{MAX}$ are the bounds of the design variable vector. Subpopulations $\mathbf{X}_{G_\varphi}$ independently and simultaneously evolve at each generation G by mutating and recombining the individuals in them to produce new subpopulations $\mathbf{U}_{G_\varphi} = [\vec{u}^1_{G_\varphi}, ..., \vec{u}^{NP}_{G_\varphi}]^T \in R^{NP\times D}$ with NP offsprings. All subpopulations $\mathbf{X}_{G_\varphi}$ present the same mutation and crossover processes as in the DE/Rand/1/Bin variant (Price et al., 2005) to create the offspring subpopulations given as indicated below:

Mutation and croosover processes

$$\vec{u}^i_{j,G_\varphi} = \begin{cases} \vec{v}^i_{j,G_\varphi} = \vec{x}^{r_{1_\varphi}}_{j,G_\varphi} + F_j(\vec{x}^{r_{2_\varphi}}_{j,G_\varphi} - \vec{x}^{r_{3_\varphi}}_{j,G_\varphi}) & \text{if } \text{rand}_j(0,1) < CR \text{ or } j = j_{rand} \\ \vec{x}^i_{j,G_\varphi} & \text{otherwise} \end{cases} \tag{21}$$

All elements of the mutant vector $\vec{v}^i_{j,G_\varphi}$ must be in its chosen bounds $[\vec{x}^i_{j,G_\varphi,MIN}, \vec{x}^i_{j,G_\varphi,MAX}]$. Any element out of its limit must be randomly generated between such limits as in the Random Position Updating Techniques described in (Juárez-Castillo, Acosta-Mesa, & Mezura-Montes, 2017). The term F_j and CR in the mutation and crossover processes refer to the scale factor and the crossover rate, respectively. In this approach the scale factor F_j is randomly generated in the interval $[0.3, 0.9]$ per each $j-th$ element of the child individual $\vec{v}^i_{G_\varphi} = [\vec{v}^i_{1,G_\varphi}, ..., \vec{v}^i_{D,G_\varphi}]^T \in R^{1\times D}$. The function $rand_j(0,1)$ is a random number generator between the interval $[0,1]$. The selection of three random individuals for the $\varphi-th$ subpopulation in the mutation process depends on the indexes $r_{1_\varphi} \in [0, NP]$, $r_{2_\varphi} \in [0, NP]$ and $r_{3_\varphi} \in [0, NP]$, where the index r_{1_φ} is called base vector index and the indexes r_{2_φ} and r_{3_φ} the difference vector indexes. Based on their fitness, the fittest individuals between the $\varphi - th$ parent subpopulation and the $\varphi - th$ child subpopulation survive and conform to the corresponding parent subpopulation to the next generation $G+1$. The above is performed by the selection process proposed in Section 3.2.1, which promotes the exploration and indirectly the exploitation of the search space and provides a spread Pareto front. Through generations, the non-dominated solutions of each generation per each subpopulation are stored in the corresponding external memories to obtain the best trade-offs from the Pareto front given through generations of each subpopulation.

In the second part of the algorithm, the non-dominated solutions of the memories are merged into a single Central External Memory $CEM \in R^{NP\times n_{CEM}}$. The mutation process is fulfilled in the neighborhood of less crowded non-dominated solutions in the central external memory. Then, the evolution of the population promotes the exploitation of scarcely explored regions of the Pareto front.

Finally, the algorithm stops once the maximum generation G_{Max} is reached. A detailed explanation of each part of the proposed MOSPDE is given below, and its pseudo-code is shown in Algorithm 1.

3.2.1. Proposed selection process promoting the spread of the Pareto front

For constrained multi-objective optimization problems, several constrained handling strategies have been proposed in the last decades (Mezura-Montes & Coello, 2011). Among the most popular and efficient constraint handling methods for the multi-objective constrained optimization problem is the Pareto-based feasible rules, to the best of the author's knowledge (Coello, 2000; Coello & Montes, 2002; Deb et al., 2002; Oyama, Shimoyama, & Fujii, 2007). In this paper, the proposed selection process between the $i-th$ parent $\vec{x}^i_{G_\varphi}$ and the child $\vec{v}^i_{G_\varphi}$ of the $\varphi-th$ subpopulations is given in Algorithm 2. The proposal is similar to (Coello & Montes, 2002; Deb et al., 2002), the main differences are that the proposed selection process explores different regions of the Pareto front (see line $5-16$ of Algorithm 2). In the first subpopulation ($\varphi=1$), a random exploration of the search space is introduced. In the second ($\varphi=2$) and third ($\varphi=3$) subpopulations, an exhaustive exploration around the two frontier regions of the Pareto front is done. Those regions promote to find non-dominated solutions that minimize J_1 and J_2, respectively. The above is achieved by selecting individuals for the mutation and crossover processes from those regions, in such a way they are exploited. Hence, the proposed selection process for the second and third subpopulations directly promotes the exploration and indirectly the exploitation (based on the mutation and crossover processes) of the furthest regions of the Pareto front, i.e., solutions that extend the spread of the Pareto front are found. For the case of the first subpopulation, only the exploration of the complete search space is done.

3.2.2. Hard and soft constraints in the mechanism design

Two definitions about the kind of constraints in the optimum mechanism design are stated in this paper: Hard constraints and soft constraints. Those definitions play an important role in the search for feasible solutions.

Definition 6. *Hard constraints: Those constraints that must be strictly satisfied through the optimization process since the non-fulfillment of such constraints results in undefined numerical values or complex numbers. For the particular problem, the hard constraints are related to the Grashof criteria (g_1-g_6 in (4)-(9)), and the valid kinematic movement ($g_{9+i}-g_{9+\bar{n}+j}$ in (13)-(14)). If those constraints are not satisfied, the design solution can not be implemented in real life.*

Definition 7. *Soft constraints: Those constraints that may be feasible or not through the optimization process, i.e., those that are not hard constraints.*

In this paper, when the performance of individuals is evaluated, hard constraints must be firstly computed. When one hard constraint is violated, the evaluation of the individual is finished assigning a very high value in both its performance function and hard/soft constraint violation number. This way of constraint evaluation reduces the computation of the performance functions and soft constraints when hard constraints are violated.

3.2.3. Promoting diversity and neighborhood exploitation of the Pareto front

The diversity and neighborhood exploitation mechanism consists of selecting different individuals in the mutation process through the optimization process, and it depends on the diversity and neighborhood exploitation factor value ($DEF \in (0, 1]$). This factor is referred to the percentage of the maximum generation number G_{Max}, where individuals of the mutation process are changed.

In the first part of the algorithm, when $G \leq (DEF * G_{Max})$, three External Memories $EM_{\varphi} \in R^{n_{EM} \times D} \ \forall \ \varphi = 1, 2, 3$ store the n_{EM} non-dominated solutions corresponding to each subpopulation. Each external memory stores individuals with different features. The first one ($EM_{\varphi=1}$) keep back those explorer non-dominated individuals (those that randomly search into the whole design space). The second one ($EM_{\varphi=2}$), house the non-dominated individuals in the feasible region around the minimization of J_1. Finally, the third one ($EM_{\varphi=3}$) stores the non-dominated individuals in the feasible region around the minimization of J_2. In this part of the algorithm, the mutation process uses (21), and the selection process is done according to Section 3.2.1. Moreover, a share and reset strategy is proposed to randomly initialize the second and third subpopulations and also to share selected information of subpopulations. This strategy is necessary to prevent premature convergence in such subpopulations. It also avoids the stagnation of solutions by promoting the exploration of the search space when initializing all individuals in both subpopulations at a specific condition, and by including a record with the furthest non-dominated solutions in subpopulations. It is considered that the furthest non-dominated solution in the memory of subpopulation $\varphi = 2$ is obtained when J_1 is more weighted, i.e., the non-dominated solution that best minimizes J_1. In the same way for the memory of subpopulation $\varphi = 3$, the furthest solution is found when J_2 is more weighted, i.e., the non-dominated solution with the minimum value of J_2. Both records of non-dominated solutions are included in the subpopulation at each reset. In Algorithm 3, the share and reset strategy is shown in detail. This strategy initializes the subpopulations and shares the best individual of each subpopulation when one of the following cases occurs: *i*) At each reset generation number G_{reset}. *ii*) When the best individual of each subpopulation through generations is repeated 5000 times. *iii*) When the individuals of the current generation have a similar fitness (based on the adaptive parameter ϵ_{φ}). It is important to note that the first subpopulation $\varphi = 1$ does not consider the share and reset strategy because when both solutions are non-dominated, the selection process, given in step 9 of Algorithm 2, induces the exploration of the search space.

In the second part of the algorithm, when $G > (DEF * G_{Max})$, three external memories are filtered to form one Central External Memory $CEM \in R^{n_{CEM} \times D}$. In the filter process, non-dominated checking is done for the three memories, and the resulting non-dominated individuals conform to the central external memory. From these three populations, the filtering process removes those solutions that are dominated by at least one solution member of the populations to form one single set of non-dominated individuals called filtered population (Villarreal-Cervantes et al., 2017). In this case, instead of using three random individuals in the mutation process from the current subpopulation, those non-dominated individuals are selected from the central external memory. In order to promote the exploitation of the neighborhood individuals of the Pareto front of CEM, the difference vector individuals ($\vec{x}^{r_{2_{\varphi}}}_{G_{\varphi}}$ and $\vec{x}^{r_{3_{\varphi}}}_{G_{\varphi}}$) in the mutation process are randomly selected around the corresponding neighborhood radius Ξ of the base vector $\vec{x}^{r_{1_{\varphi}}}_{G_{\varphi}}$. The neighborhood radius Ξ is the percentage of individuals in the

central external memory, which are located around the base vector in the phenotype space. This procedure is detailed in Algorithm 4.

Also, the diversity of the Pareto front is increased due to the base vector $\vec{x}_{G_\varphi}^{r_{1\varphi}}$ must be randomly selected in a lesser crowded region of the central external memory. The individuals of the crowded region are obtained by using the crowding distance (Deb et al., 2002). Then, the base vector is selected from the 50% of population individuals in the lesser crowded region. The crowding distance of the $i-th$ individual is half of the perimeter of a rectangle formed by the vertices, which include the $(i-1)-th$ individual and the $(i+1)-th$ individual in the phenotype space. The individual with a more significant value of this distance measure is less crowded by other solutions. Hence, the selection of difference vector individuals in the neighborhood radius of the base solution increases the search into a specific unexplored and less crowded region of the phenotype space. On the other hand, the selection process is proposed between the $i-th$ generated child and its base vector. The only difference in the selection process given in the first part of the algorithm is when both individuals are not non-dominated feasible solutions (see step 15 of Algorithm 2). In this case, the child vector is preferred due to the base vector already belongs to the central external memory.

The switching mechanism of the proposed algorithm, which is controlled by the DEF parameter, promotes two behaviors:

- The first part of the search aims to promote the exploration of the whole search space by using random individuals into the first subpopulation and also the exploration and exploitation of furthest regions of the Pareto front by using the second and third subpopulations. These three subpopulations provide spread Pareto solutions.
- The second part of the algorithm focuses on the exploitation of the less crowded region of the previously found non-dominated individuals. This process benefits to find more non-dominated solutions in scarcely explored regions of the Pareto front.

3.2.4. External memories

As commented previously, three external memories $EM_\varphi \ \forall \ \varphi = 1, 2, 3$ are set in the first part of the algorithm ($G \leq (DEF * G_{Max})$). Those memories store the corresponding non-dominated solutions through the generation of subpopulations (one memory per each subpopulation). Hence, for each subpopulation memory, the Pareto fronts obtained in the current and previous generations (G and $G-1$, respectively) are filtered together. Therefore, the external memories are used to obtain the best trade-offs from the Pareto front through generations. In the second part of the algorithm ($G > (DEF * G_{Max})$), the three memories are filtered to form the Central External Memory CEM to obtain a spread Pareto front.

On the other hand, the external memories EM and the central external memory CEM allow a maximum number of individuals of n_{EM} and n_{CEM}, respectively. If the non-dominated individuals in the memories exceed the maximum number permitted, then a sudden extinction mechanism (SEM) is used to eliminate the rest of the individuals. The sudden extinction mechanism promotes the removal of individuals from the more crowded regions to preserve diversity. The SEM reduces the computation time of the algorithm when the filter process is done. This procedure is detailed in the pseudo-code

showed in Algorithm 5.

4. Results

The result analysis consists of comparing the performance of three multi-objective search approaches in the dimensional synthesis of the mechanism for bipedal gait generation. This comparison includes seven state-of-art multi-objective optimizers and the proposed multi-objective specialist population-based differential evolution algorithm (MOSPDE). The main characteristic of these optimizers is the search approach. Four approaches are based on Pareto dominance, and the last two are related to the decomposition-based and metric-driven search approaches, respectively. The Pareto dominance approaches include the Multi-Objective Differential Evolution (MODE) (Price et al., 2005), the Multi-Objective Differential Evolution with reconfigurability promotion by a crowding mechanism (CR-MODE) (Portilla-Flores et al., 2011), the Multi-Objective Exhaustive Exploitation Differential Evolution (MOEEDE) (Villarreal-Cervantes, 2017), the Non-dominated Sorting Genetic Algorithm II (NSGAII) (Deb et al., 2002), and the Multiple Objective Particle Swarm Optimization (MOPSO) (Coello et al., 2004); the one related to the decomposition metric-driven search approach is the Multi-objective Evolutionary Algorithm based on Decomposition and Differential Evolution (MOEA-D) (Zhang & Li, 2007); and the last algorithm is the S-Metric Selection Evolutionary Multi-objective Algorithm (SMS-EMOA) (Beume et al., 2007), which is based on a metric-driven search approach. The selection of these algorithms is because they could give a well-distributed set of Pareto solutions with different search approaches.

A stop criterion is set to the number of objective function evaluations to provide fair comparisons. Then, the evaluation number is $EN = 10E6$. The population size for those algorithms that include external memory (external archive or repository) is $NP = 20$; this is the case of MODE, CR-MODE, MOEEDE, MOPSO, and the proposed MOSPDE. For the NSGA-II, the population size is set as $NP = 100$, and for the MOEA/D-DE and the SMS-EMOA is $NP = 200$. The maximum capacity in the external memory is three hundred individuals. For those algorithms that do not require external memory in search of solutions (NSGA-II, MOEA/D-DE, SMS-EMOA), the non-dominated solutions of the last generation in the population are stored in a memory.

The rest of the parameters of the multi-objective optimizers are shown in Table 3 and selected accordingly to the recommendation proposed in the corresponding multi-objective technique.

4.1. Algorithm performance analysis

Thirty independent runs are performed per each algorithm using a PC with a 3.5 GHz Intel Core(TM) i7-4770K processor and 32GB of RAM. The empirical analysis is based on the quality features of the obtained Pareto front per each algorithm. Two of the most important performance metrics measure the quality (Jiang, Ong, Zhang, & Feng, 2014) considering normalized objective functions and the true Pareto front $\mathcal{PF}^*$. Such front is considered as the Pareto front approximation $\mathcal{PF}^A$ given by all non-dominated solutions through all algorithm runs (filtered of all runs). The Nadir and

the Ideal objective vectors of the normalized objective functions were found through all algorithm runs. The performance metrics are *i*) Based on Capacity: The Overall Non-dominated Vector Generation (ONVG) and *ii*) Based on Diversity and Convergence: The Hyper-Volume (HV). In the case of the HV, the Nadir vector is selected as the reference point.

The descriptive statistic of each quality measure per multi-objective optimizer is summarized in Table 4 where the columns with the terms $mean(\star)$ and $\sigma(\star)$ indicate the average and the standard deviation of the performance metric "$\star$", respectively; the column CT is related to the convergence time of the algorithm. One sample of the descriptive statistics is related to the performance metric of the obtained Pareto front per each algorithm run. On the other hand, to draw general conclusions about the algorithm performance (reliability of the results), non-parametric inferential statistical tests (Derrac et al., 2011) are applied to the results obtained in the samples of runs per each algorithm. As a first step, the 95%-confidence Friedman test is applied to prove the existence of significant differences among the quality of the obtained Pareto front in the multi-objective optimizer, and hence, to determine if one algorithm outperforms the other. According to the returned $p-value$ shown in Table 5, there are significant differences among runs with a confidence of 99.99%. Then, the Friedman test for multiple comparisons with the most representative post-hoc error correction methods is carried out for finding the accurate pairwise comparisons. Tables 6 and 7 present the unadjusted $p-value$ from the Friedman test, and its corrected values obtained by the Holm, Shaffer, and Bergmann methods for all particular comparisons. Also, those tables show the number of wins in boldface based on the statistical significance and the Friedman rank ($z-value$). Regarding the descriptive and inferential statistics in the corresponding tables, different findings are observed:

- The algorithm MOSPDE is the most promising optimizer in the optimal synthesis of the eight-bar mechanism for the bipedal gait generation because:
  a) It provides the best diversity and convergence of the obtained Pareto front. The above is verified for the specific sample by the descriptive statistical data concerning the Hyper-Volume in Table 4, and by the generalization given in Table 6, which confirms the outstanding performance with a 99.99% of confidence in the results when MOSPDE wins. These results also indicate that the exploration around the frontier regions of the Pareto front, given by the proposed selection process mechanism in subpopulations, promotes the spread of the obtained solutions. Moreover, the DEF (diversity and neighborhood exploitation factor) enhances the diversity and convergence of the Pareto front by exploiting, through the search, non-dominated solutions in scarcely explored regions.
  b) It obtains the 93.71% of the maximum non-dominated solutions in the external memory, as is shown in the column $mean(ONVG)$ of Table 4. Based on the results regarding the ONVG metric in Table 7, the MOSPDE presents one of the best performances (as in the case of MOEEDE and MOPSO) related to the search of non-dominated solutions. This behavior is attributed to the exploitation of less crowded Pareto front regions given by the second part of the algorithm, which promotes the search of unexplored search space areas.

- MOEEDE follows MOSPDE in performance because it obtains the second-best Pareto front concerning the diversity and convergence based on HV, and also the best quality indicator in the ONVG metric with a 99.99% confidence in the results when MOEEDE wins. Also, the descriptive statistical data indicates that

it can find the 98% of the maximum non-dominated solutions in the external memory.

- The lowest-performing algorithm is the MOPSO because it finds a Pareto front with several solutions with the worst convergence and diversity based on the HV metric. Also, this algorithm presents the most considerable convergence time.
- There is a relation between the convergence time and the improvement in the quality of the Pareto front achieved by multi-objective optimizers. Based on the CT column in Table 4, the MOSPDE presents the second largest convergence time, followed by MOEEDE, and they are the first and the second most suitable algorithms, respectively. The above is due to both algorithms use mechanisms to increase the exploitation of non-dominated solutions through generations: The former (proposal) by a diversity and neighborhood exploitation mechanism through subpopulations, and the latter, by an exhaustive exploitation mechanism through a hyper-grid, then an increment of the convergence time is observed.
- The algorithms MOEA/D-DE and SMS-EMOA do not present convincing results in the HV metric, i.e., these algorithms can not find Pareto fronts with better diversity and convergence. Nevertheless, based on the ONVG metric, they can find the 66.66% of the maximum non-dominated solutions in the external memory (obtaining the second place concerning ONVG). Nevertheless, it is essential to point out that the memory of both algorithms is bounded by the population size $NP = 200$. So, those algorithms find the maximum number of non-dominated solutions related to the number of individuals in the population.

Additionally, to know the resulting Pareto front obtained by all runs of the multi-objective optimizer, the thirteen fronts obtained by runs are filtered into a single front, and those are visualized in Fig. 2. The values of the Hiper-Volume, the Overall Non-dominated Vector Generation, and the two-set-coverage metric (C-metric) for the filtered front are given in Tables 8 and 9, respectively. Based on those results, some findings are stated:

- The most outstanding performance is provided by the proposal MOSPDE because it can obtain a filtered Pareto front with more diversity and convergence (see the HV values in Table 8). Also, this can find a suitable number of non-dominated solutions, as confirmed with the ONVG metric (third-best place). The second best optimizer is MOEEDE, followed by SMS-EMOA, CR-MODE, NSGA-II, MOEA/D-DE, MODE, and MOPSO regarding the HV metric.
- According to the number of wins in pairwise comparisons between algorithm solutions for the C-metric, the algorithm that covers more than other algorithms (best coverage) is MOEA/D-DE with seven wins. The proposal MOSPDE follows MOEA/D-DE with six wins, MOEEDE with five, CR-MODE with four, NSGAII with three, SMS-EMOA with two, MODE with one, and MOPSO without any. The only comparative case where the proposal MOSPDE is not superior in the C-metric is when it is compared to MOEA/D-DE. The solutions of MOEA/D-DE dominate 22.59% of the ones obtained by MOSPDE; meanwhile, the solutions of MOSPDE dominate 1.60% of the corresponding ones of MOEA/D-DE. Nevertheless, the solutions in MOEA/D-DE mainly dominate a small inferior part of the Pareto front (the inferior region as is observed in Fig. 2) where there are not suitable trade-offs for the bipedal locomotion with the eight-bar mechanism. On the other hand, the proposal solutions dominate the superior region of the

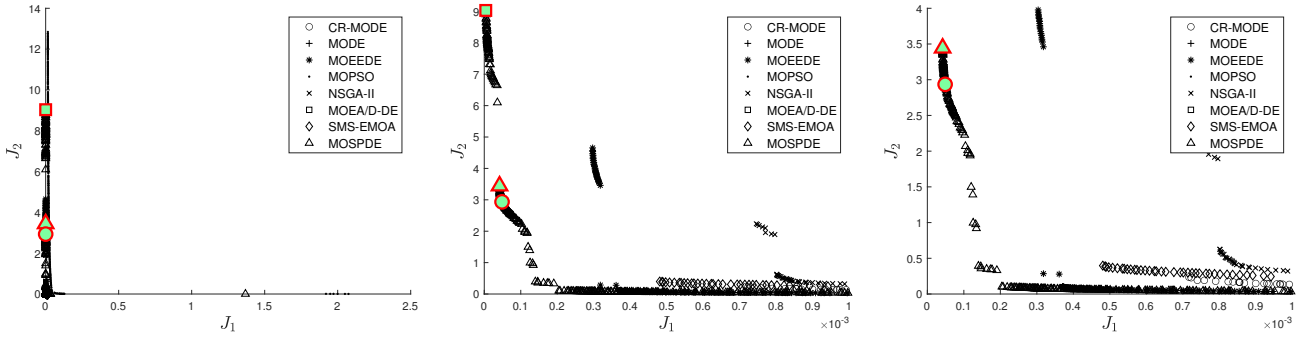

a) Original figure. b) Figure with different close-up views.

Figure 2.: Filtered Pareto front of the multi-objective optimizers.

Pareto front, where better design trade-offs appeared, and only in that region exists 5.60% of the MODE solutions. The above indicates that using specialist subpopulations that cover different regions of the Pareto front promotes the exploration of the search space and the exploitation of specific areas of the Pareto front. In this way, a broad set of non-dominated solutions is found in the whole Pareto front. Then, more reconfigurability of the eight-bar mechanism can be obtained to perform the bipedal locomotion.

4.2. Design performance analysis

In this section, the design solutions with two specific trade-offs for the most representative obtained filtered Pareto fronts are analyzed. Those trade-off solutions are obtained from the best multi-objective optimizer MOSPDE (proposal). The corresponding solutions named as x^{t*}_{MOSPDE} and x^{c*}_{MOSPDE} are located in a similar region of the filtered Pareto front, both observed as a big triangle $f^*_1(x^{t*}_{MOSPDE})$ and a circle $f^*_2(x^{c*}_{MOSPDE})$ in Fig. 2. An additional solution is also included; this represents the extreme of the Pareto front obtained by the proposal MOSPDE, where the solution minimizes further the trajectory tracking. This solution is named as x^{*EXT}_{MOSPDE} and displayed as a big square in Fig. 2. With this experiment, the importance of improving the search in the multi-objective algorithms for complex problems, which results in more useful design solutions (trade-offs), can be highlighted based on the information about the significant performance differences between selected solutions ..

In Table 10, the performance functions and the design variable vectors of the selected trade-offs are displayed, and also in Fig. 3 the schematic representations and the generated paths of such designs are shown. Based on those designs, different findings are highlighted:

- The design x^{t*}_{MOSPDE} can achieve the trade-off in the point tracking of $f^*_1(\vec{x}^{t*}_{MOSPDE}) = 4.189E-5$ and in the force transmission of $f^{t*}_2(\vec{x}^{t*}_{MOSPDE}) = 3.443$, while the design x^{c*}_{MOSPDE} achieves the trade-off $f^*_1(\vec{x}^{c*}_{MOSPDE}) = 4.869E-5$ and $f^*_2(\vec{x}^{c*}_{MOSPDE}) = 2.935$. The first design ($x^{t*}_{MOSPDE}$) can improve the accuracy in around 13.97% and deteriorate the force transmission in around 14.75% concerning the second design x^{c*}_{MOSPDE}. The contrary happens with the second design when compared to the first one. Also, the former presents a maximum Euclidean distance tracking error of $0.0033m$, while the latter has an error

of $0.0037m$. Although the selected lower-limb mechanism design trade-offs are close to each other, they present different benefits that can be useful in a particular application. The above indicates that using subpopulations and information exchange operations in MPSPDE benefits the exploration and exploitation of different regions of the Pareto front and enhances the reconfigurability in the design.

- In the case that the most important condition was the trajectory tracking, the best design concerning it, is given by the extreme of the Pareto front obtained by MOSPDE x^{*EXT}_{MOSPDE} ($f^*_1(\vec{x}^{*EXT}_{MOSPDE}) = 4.1E-6$). This design carries out the point tracking with a maximum Euclidean distance error of $0.0015m$ (a reduction of around half compared to other design trade-offs). Nevertheless, it presents the worst force transmission ($f^*_2(\vec{x}^{*EXT}_{MOSPDE}) = 9.031$). The deterioration of the force transmission is 61.87%, while the improvement of the tracking error is 90.19% concerning the design x^{t*}_{MOSPDE}. The above indicates that both design objectives are in conflict, and the solutions around the selected trade-off, marked with a triangle in the Pareto front of Fig. 2, provide the most promising design reconfigurability (which suitable balance both performance functions) in the eight-bar mechanism for the bipedal locomotion.

- There is a clear trade-off between trajectory tracking and force transmission, i.e., improving trajectory tracking implies reducing force transmission and vice versa. The most suitable mechanism for the bipedal gait generation not only depends on the trajectory tracking but also on the force transmission exerted in the stance phase. The results indicate the importance of the study of efficient search strategies which promote the reconfigurability (trade-offs) in the lower-limb mechanism design. In this sense, for a real scenario, where the best design configuration for the specific application is not known (which is assumed in real-world optimization problems), the decision-maker may select a not so good design if the optimizer can not find a broad set of solutions.

Finally, the Computer-Aided Design (CAD) of the selected design solution x^{t*}_{MOSPDE} obtained by the MOSPDE is shown in Fig. 4. It can be observed that the eight-bar mechanism can perform the small-scaled human gait with a suitable force transmission, as indicated in Table 10. A video of the movement of the selected design for the eight-bar mechanism in a specific routine of bipedal locomotion is given in the following link: `https://www.dropbox.com/sh/vagy41l7vk2i6e2/AAB99WvGkw0blma3CUbiQ0eka?dl=0`

5. Conclusion

In this paper, the reconfigurability of the eight-bar mechanism for bipedal gait stated as a discrete-continuous multi-objective dimensional synthesis optimization problem is studied by comparing three different multi-objective search approaches (dominance-based, decomposition-based and metric-driven) by using seven state-of-the-art MHAs.

The statistical evidence indicates that the dominance-based search approach (MOSPDE and MOEEDE) guides the search to the most promising solutions, i.e., the obtained Pareto front presents a better convergence, diversity, and more non-dominated solutions based on the HV and ONVG metrics. The two most representative algorithms (MOSPDE and MOEEDE) share the following characteristics: Both include dominance-based search approaches and also exploitation strategies of different regions

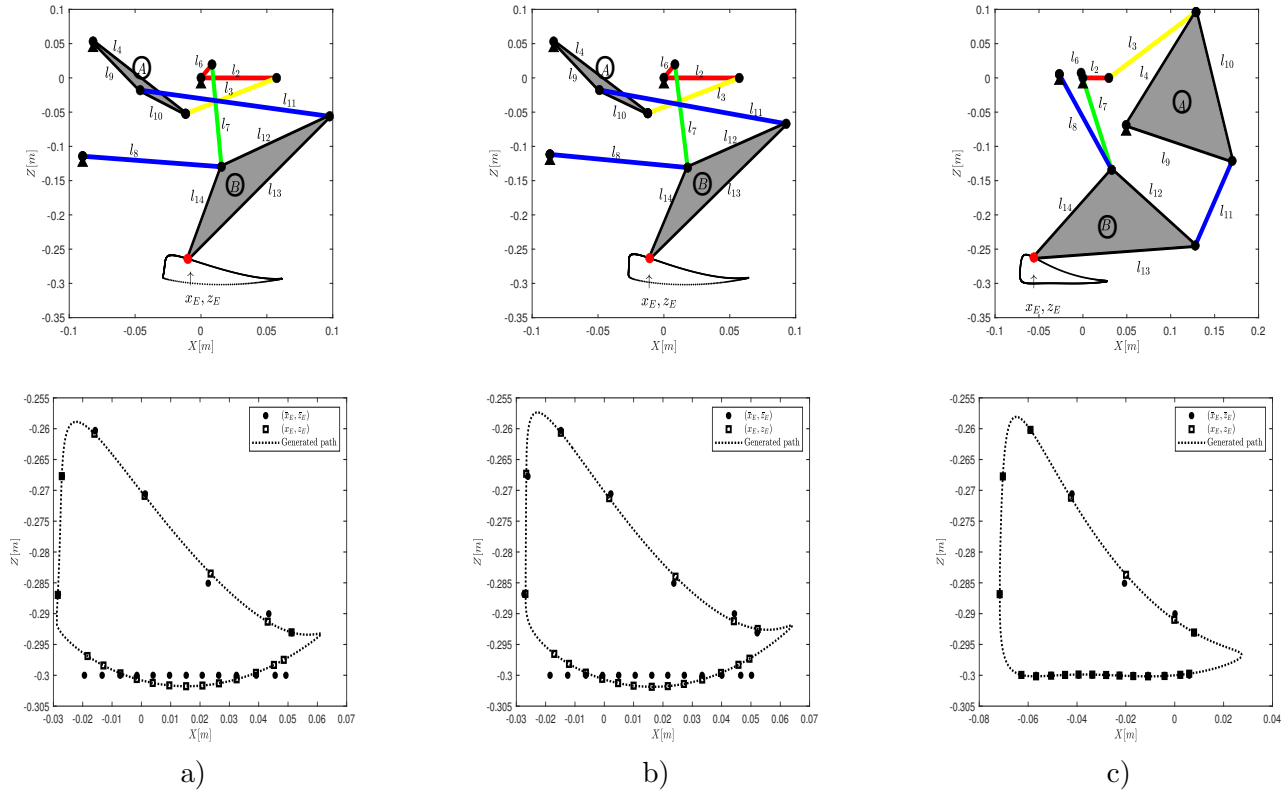

a) b) c)

Figure 3.: Obtained designs and generated paths for three specific trade-offs in the two most representative multi-objective optimizers. a) $\vec{x}^{t*}_{MOSPDE}$. b) $\vec{x}^{c*}_{MOSPDE}$. c) $\vec{x}^{*EXT}_{MOSPDE}$.

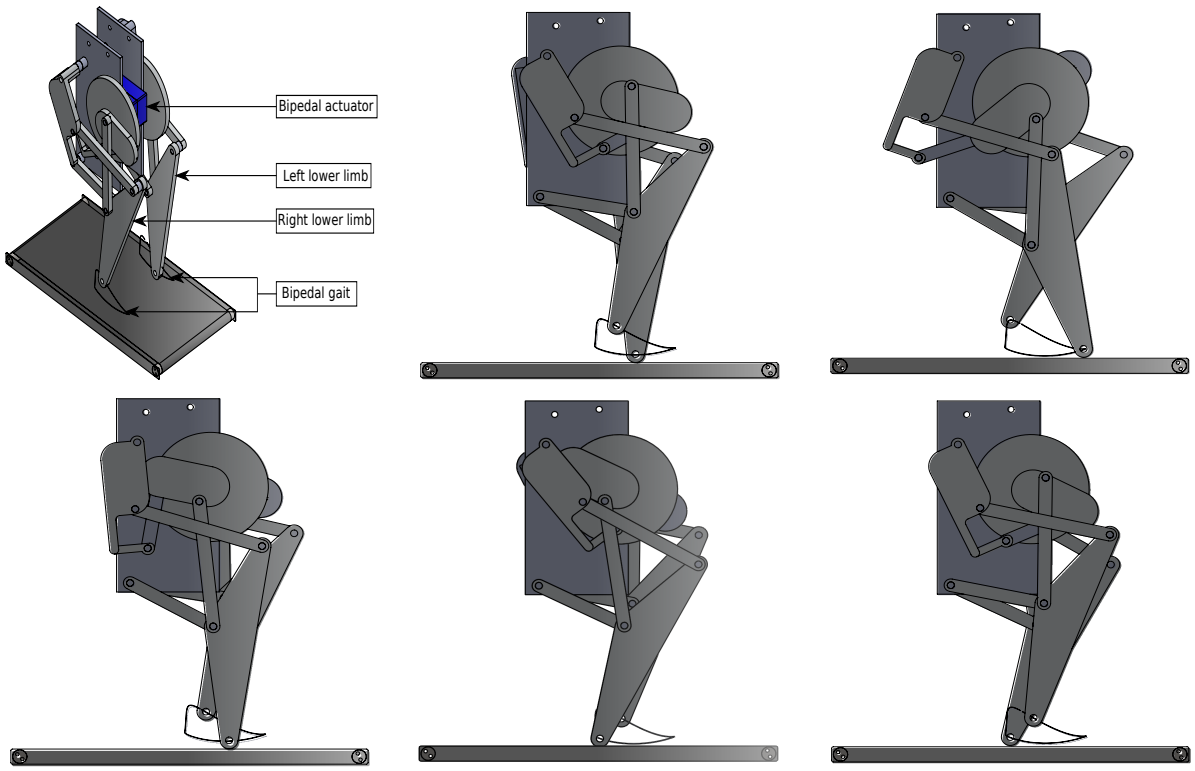

Figure 4.: CAD of the bipedal lower-limb based on the eight-bar mechanism design $\vec{x}^{t*}_{MOSPDE}$.

of the Pareto front. The above indicates that the dominance-based search approach with efficient exploitation of non-dominated solutions per Pareto region improves the diversity, convergence, and the number of non-dominated solutions in the dimensional synthesis of the eight-bar mechanism.

The decomposition and metric-driven search approaches share the characteristic of finding a suitable number of non-dominated solutions (all individuals in the population are non-dominated). However, they lack strategies to improve the Pareto front in the dimensional synthesis of the eight-bar bipedal gait generation mechanism.

According to the C-metric, the statistical evidence shows that decomposition and dominance-based search approaches (MOEA/D-DE, MOSPDE, and MOEEDE) can show better coverage. In particular, MOEA/D-DE provides the best coverage, followed by MOSPDE and MOEEDE. Nevertheless, the decomposition search approach (MOEA/D-DE) only covers a small inferior part of the Pareto front, where the trade-offs are not viable for the application in the bipedal gait. Then, having proper coverage does not mean a suitable Pareto front. A balance among coverage, diversity, and convergence is required to find the best quality of the approximated Pareto front.

The proposed dominance-based search algorithm MOSPDE presents outstanding performance concerning the other optimizers because this offers the best diversity and convergence of the Pareto front with a suitable number of non-dominated solutions and also with a more spread Pareto front due to its coverage. This fact is attributed to the inclusion of Pareto dominance to guide the search to the best trade-off among solutions, the use of specialist subpopulations that cover different regions of the Pareto front promoting the exploration of the search space and the exploitation of specific regions of the Pareto front, and the information exchange among subpopulations. Those facts promote major design reconfigurability of the eight-bar mechanism with different trade-offs to perform the bipedal locomotion.

An important fact to improve the trade-offs in the dimensional synthesis of the bipedal locomotion mechanism is the exploitation characteristic of the optimizer. Future works involve the use of hybrid strategies with local search approaches to finely search through specific Pareto regions and also the application of the MOSPDE in the dimensional synthesis of other types of mechanisms.

Disclosure statement

No potential conflict of interest was reported by the authors.

Funding

This work was supported in part by the Secretaría de Investigación y Posgrado (SIP) under the project grant number 20180196.

Notes on contributors

Miguel Gabriel Villarreal-Cervantes received his B.S. degree in Electronic Engineering from the Veracruz Technological Institute, Veracruz, Mexico, in 2003, and the M.Sc. and

Ph.D. degrees in Electrical Engineering from the Center for Research and Advanced Studies, CINVESTAV, Mexico City, Mexico, in 2005 and 2010, respectively. He is a Full Professor within the Postgraduate Department of the "Centro de Innovación y Desarrollo Tecnológico en Cómputo del Instituto Politécnico Nacional" (CIDETEC-IPN) in Mexico City where he directs the Optimal Mechatronic Design Laboratory. He is a member of the National System of Researchers and the Expert Network on Robotics and Mechatronics, IPN (ENRM-IPN). He was the Head of the Mechatronic Section in the CIDETEC-IPN, from 2013 to 2016, and the ENRM-IPN, from 2012 to 2017. His current research interests include mechatronic design based on optimization (mono and multiobjective optimization), bio-inspired metaheuristics in the optimal mechatronic design, optimal tuning for the mechatronic system control based on metaheuristic algorithms (offline and online strategies), and robotics.

Jesús Said Pantoja-García received the B.S. degree in automation and control engineering from the National Polytechnic Institute (IPN), Mexico in 2013, the M.S. in computer technology from the "Centro de Innovación y Desarrollo Tecnológico en Cómputo" of the IPN (CIDETEC-IPN) in 2015 and the Ph.D. in robotics and mechatronic systems engineering at the Centro de Innovación y Desarrollo Tecnológico en Cómputo (CIDETEC) of the IPN in 2019. He is currently a professor at Universidad Tecnológica de México – UNITEC MÉXICO. He has been interested in the optimal mechanism design by using single-objective and multi-objective optimization approaches. His main fields are the application of meta-heuristics techniques in mechatronic, synergetic design, and dynamic modeling.

Alejandro Rodríguez-Molina received the B.S. degree in computer systems engineering from the Escuela Superior de Cómputo (ESCOM) of the Instituto Politécnico Nacional (IPN) in 2013, the M.Sc. in computer science from the Centro de Investigación y de Estudios Avanzados (CINVESTAV) of the IPN in 2015, and the Ph.D. in robotics and mechatronic systems engineering at the Centro de Innovación y Desarrollo Tecnológico en Cómputo (CIDETEC) of the IPN in 2019. He is currently a full-time professor at the research and postgraduate division in the Instituto Tecnológico de Tlalnepantla (ITTLA) of the Tecnológico Nacional de México (TecNM). His research interests are the design and implementation of bio-inspired meta-heuristics for optimization and their application to engineering problems.

Saul Enrique Benitez-Garcia received the B.S. degree in Communication and Electronic Engineering from Escuela Superior de Ingeniería Mecánica y Eléctrica (ESIME) of the Instituto Politécnico Nacional (IPN) in 2019 and received the M.Sc. degree in Computer Technology from Centro de Innovación y Desarrollo Tecnológico en Cómputo (CIDETEC) of the IPN in 2019. He is currently pursuing the Ph.D. degree in Robotic and Mechatronic Systems Engineering with the CIDETEC of the IPN. His research interests include control systems, optimization of mechatronic systems and hardware implementation.

References

Alexander, R. M. (1990). Three uses for springs in legged locomotion. *The International Journal of Robotics Research*, *9*(2), 53-61.

Aliman, N., Ramli, R., & Haris, S. (2017). Design and development of lower limb exoskeletons: A survey. *Robotics and Autonomous Systems*, *95*, 102 - 116.

Aoustin, Y., & Hamon, A. (2013). Human like trajectory generation for a biped robot with a four-bar linkage for the knees. *Robotics and Autonomous Systems*, *61*(12), 1717 - 1725.

Arcos-Legarda, J., Cortes-Romero, J., & Tovar, A. (2019). Robust compound control of dynamic bipedal robots. *Mechatronics*, *59*, 154 - 167.

Balli, S. S., & Chand, S. (2002). Transmission angle in mechanisms (triangle in mech). *Mechanism and Machine Theory*, *37*(2), 175–195.

Bazaraa, M. S., Sherali, H. D., & Shetty, C. M. (2006). *Nonlinear programming: Theory and algorithms*. Wiley-Interscience.

Beume, N., Naujoks, B., & Emmerich, M. (2007). Sms-emoa: Multiobjective selection based on dominated hypervolume. *European Journal of Operational Research*, *181*(3), 1653 - 1669.

Bovi, G., Rabuffetti, M., Mazzoleni, P., & Ferrarin, M. (2011). A multiple-task gait analysis approach: kinematic, kinetic and emg reference data for healthy young and adult subjects. *Gait & posture*, *33*(1), 6–13.

Bulatović, R. R., Dordević, S. R., & Dordević, V. S. (2013). Cuckoo search algorithm: A metaheuristic approach to solving the problem of optimum synthesis of a six-bar double dwell linkage. *Mechanism and Machine Theory*, *61*, 1 - 13.

Bulatović, R. R., Miodragović, G., & Bošković, M. S. (2016). Modified krill herd (mkh) algorithm and its application in dimensional synthesis of a four-bar linkage. *Mechanism and Machine Theory*, *95*, 1 - 21.

Cabrera, J., Nadal, F., Muñoz, J., & Simon, A. (2007). Multiobjective constrained optimal synthesis of planar mechanisms using a new evolutionary algorithm. *Mechanism and Machine Theory*, *42*(7), 791 - 806.

Chanekar, P. V., Fenelon, M. A. A., & Ghosal, A. (2013). Synthesis of adjustable spherical four-link mechanisms for approximate multi-path generation. *Mechanism and Machine Theory*, *70*, 538 - 552.

Coello, C. A. C. (2000). Constraint-handling using an evolutionary multiobjective optimization technique. *Civil Engineering and Environmental Systems*, *17*(4), 319-346.

Coello, C. A. C., Lamont, G. B., & Veldhuizen, D. A. V. (2007). *Evolutionary algorithms for solving multi-objective problems*. Springer.

Coello, C. A. C., & Montes, E. M. (2002). Constraint-handling in genetic algorithms through the use of dominance-based tournament selection. *Advanced Engineering Informatics*, *16*(3), 193 - 203.

Coello, C. A. C., Pulido, G. T., & Lechuga, M. S. (2004). Handling multiple objectives with particle swarm optimization. *IEEE Transactions on Evolutionary Computation*, *8*(3), 256-279.

Corne, D. W., & Knowles, J. D. (2003). No free lunch and free leftovers theorems for multiobjective optimisation problems. In *Proceedings of the 2nd international conference on evolutionary multi-criterion optimization* (pp. 327–341).

Deb, K., Pratap, A., Agarwal, S., & Meyarivan, T. (2002). A fast and elitist multiobjective genetic algorithm: Nsga-ii. *IEEE Transactions on Evolutionary Computation*, *6*(2), 182-197.

Derrac, J., García, S., Molina, D., & Herrera, F. (2011). A practical tutorial on the use of nonparametric statistical tests as a methodology for comparing evolutionary and swarm intelligence algorithms. *Swarm and Evolutionary Computation*, *1*(1), 3 - 18.

Ebrahimi, S., & Payvandy, P. (2015). Efficient constrained synthesis of path generating four-bar mechanisms based on the heuristic optimization algorithms. *Mechanism and Machine Theory*, *85*, 189 - 204.

EL-Kribi, B., Houidi, A., Affi, Z., & Romdhane, L. (2013). Application of multi-objective genetic algorithms to the mechatronic design of a four bar system with continuous and discrete variables. *Mechanism and Machine Theory*, *61*, 68 - 83.

Garcia-Saura, C. (2015). *Central pattern generators for the control of robotic systems.*

Gui, S. (2019). Identification design of one-dof eight-bar based on limb movements. *Mechanism and Machine Theory*, *142*, 103592.

Ito, S., Nishio, S., Ino, M., Morita, R., Matsushita, K., & Sasaki, M. (2018). Design and adaptive balance control of a biped robot with fewer actuators for slope walking. *Mechatronics*, *49*, 56 - 66.

Jiang, S., Ong, Y., Zhang, J., & Feng, L. (2014). Consistencies and contradictions of performance metrics in multiobjective optimization. *IEEE Transactions on Cybernetics*, *44*(12), 2391-2404.

Juárez-Castillo, E., Acosta-Mesa, H., & Mezura-Montes, E. (2017). Empirical study of bound constraint-handling methods in particle swarm optimization for constrained search spaces. In *2017 ieee congress on evolutionary computation (cec)* (p. 604-611).

Kajita, S., Hirukawa, H., Harada, K., & Yokoi, K. (2014). *Introduction to humanoid robotics*. Springer Publishing Company, Incorporated.

Khorshidi, M., Soheilypour, M., Peyro, M., Atai, A., & Panahi, M. S. (2011). Optimal design of four-bar mechanisms using a hybrid multi-objective ga with adaptive local search. *Mechanism and Machine Theory*, *46*(10), 1453 - 1465.

Lim, I., Kwon, O., & Park, J. H. (2014). Gait optimization of biped robots based on human motion analysis. *Robotics and Autonomous Systems*, *62*(2), 229 - 240.

Lin, W.-Y. (2010). A ga–de hybrid evolutionary algorithm for path synthesis of four-bar linkage. *Mechanism and Machine Theory*, *45*(8), 1096 - 1107.

Matos, V., & Santos, C. P. (2014). Towards goal-directed biped locomotion: Combining cpgs and motion primitives. *Robotics and Autonomous Systems*, *62*(12), 1669 - 1690.

Mehdigholi, H., & Akbarnejad, S. (2012). Optimization of watt's six-bar linkage to generate straight and parallel leg motion. *International Journal of Advanced Robotic Systems*, *9*, 1-7.

Mezura-Montes, E., & Coello, C. A. C. (2011). Constraint-handling in nature-inspired numerical optimization: Past, present and future. *Swarm and Evolutionary Computation*, *1*(4), 173 - 194.

Nariman-Zadeh, N., Felezi, M., Jamali, A., & Ganji, M. (2009). Pareto optimal synthesis of four-bar mechanisms for path generation. *Mechanism and Machine Theory*, *44*(1), 180 - 191.

Ortiz, A., Cabrera, J., Nadal, F., & Nadal, A. (2013). Dimensional synthesis of mechanisms using differential evolution with auto-adaptive control parameters. *Mechanism and Machine Theory*, *64*, 210 - 229.

Osycska, A. (1984). Multi-criterion optimization in engineering with for-tran examples. John Wiley & Sons.

Oyama, A., Shimoyama, K., & Fujii, K. (2007). New constraint-handling method for multi-objective and multi-constraint evolutionary optimization. *Transactions of the japan society for aeronautical and space sciences*, *50*(167), 56-62.

Pantoja-García, J., Villarreal-Cervantes, M., González-Robles, J., & Cervantes, G. S. (2017). Síntesis óptima de un mecanismo para la marcha bípeda utilizando evolución diferencial. *Revista Internacional de Métodos Numéricos para Cálculo y Diseño en Ingeniería*, *33*(1), 138 - 153.

Pinto, C. M. A., & Golubitsky, M. (2006). Central pattern generators for bipedal locomotion. *J Math Biol*, *53*(3), 474-489.

Portilla-Flores, E. A., Mezura-Montes, E., Alvarez-Gallegos, J., Coello-Coello, C. A., Cruz-Villar, C. A., & Villarreal-Cervantes, M. G. (2011). Parametric reconfiguration improvement in non-iterative concurrent mechatronic design using an evolutionary-based approach. *Engineering Applications of Artificial Intelligence*, *24*(5), 757 - 771.

Price, K., Storn, R. M., & Lampinen, J. A. (2005). *Differential evolution: A practical approach to global optimization*. Springer.

Reynoso-Meza, G., Blasco, X., Sanchis, J., & Martínez, M. (2014). Controller tuning using evolutionary multi-objective optimisation: Current trends and applications. *Control Eng Pract*, *28*, 58 - 73.

Richter, H., Simon, D., Smith, W. A., & Samorezov, S. (2015). Dynamic modeling, parameter estimation and control of a leg prosthesis test robot. *Applied Mathematical Modelling*, *39*(2), 559 - 573.

Russo, M., Herrero, S., Altuzarra, O., & Ceccarelli, M. (2018). Kinematic analysis and multi-objective optimization of a 3-upr parallel mechanism for a robotic leg. *Mechanism and Machine Theory*, *120*, 192 - 202.

Sancibrian, R., Sarabia, E. G., Sedano, A., & Blanco, J. M. (2016). A general method for the optimal synthesis of mechanisms using prescribed instant center positions. *Applied Mathematical Modelling*, *40*(3), 2206 - 2222.

Sandor, G. N., & Erdman, A. (1984). *Advanced mechanism design, analysis and synthesis*. Prentice-Hall.

Sarkar, A., & Dutta, A. (2015). 8-dof biped robot with compliant-links. *Robotics and Autonomous Systems*, *63, Part 1*(0), 57 - 67.

Shao, Y., Xiang, Z., Liu, H., & Li, L. (2016). Conceptual design and dimensional synthesis of cam-linkage mechanisms for gait rehabilitation. *Mechanism and Machine Theory*, *104*, 31 - 42.

Sleesongsom, S., & Bureerat, S. (2017). Four-bar linkage path generation through self-adaptive population size teaching-learning based optimization. *Knowledge-Based Systems*, *135*, 180 - 191.

Tsuge, B. Y., Plecnik, M. M., & McCarthy, J. M. (2016). Homotopy directed optimization to design a six-bar linkage for a lower limb with a natural ankle trajectory. *ASME. J. Mechanisms Robotics*, *8*(6), 061009-061009-7.

Uicker, J., Pennock, G., & Shigley, J. (2010). *Theory of machines and mechanisms*. Oxford University Press.

Ávila Hernández, P., & Cuenca-Jiménez, F. (2018). Design and synthesis of a 2 dof 9-bar spatial mechanism for a prosthetic thumb. *Mechanism and Machine Theory*, *121*, 697 - 717.

Villarreal-Cervantes, M. G. (2017). Approximate and widespread pareto solutions in the structure-control design of mechatronic systems. *Journal of Optimization Theory and Applications*, *173*(2), 628–657.

Villarreal-Cervantes, M. G., Rodríguez-Molina, A., García-Mendoza, C. V., Peñaloza-Mejía, O., & Sepúlveda-Cervantes, G. (2017). Multi-objective on-line optimization approach for the dc motor controller tuning using differential evolution. *IEEE Access*, *5*, 20393-20407.

Vukobratovic, M., & Borovac, B. (2004). Zero-moment point - thirty five years of its life. *Int. J. Humanoid Robotics*, *1*, 157-173.

Waldron, K. J., Kinzel, G., & Agrawal, S. K. (2016). *Kinematics, dynamics, and design of machinery*. Wiley.

Wang, F. C., Yu, C. H., Chou, T.-Y., & Chang, N.-C. (2009). Design and control of an active gait trainer. In *2009 ieee international symposium on industrial electronics* (p. 1779-1784).

Yang, L., Liu, Z., & Chen, Y. (2019). Energy efficient walking control for biped robots using interval type-2 fuzzy logic systems and optimized iteration algorithm. *ISA Transactions*, *87*, 143 - 153.

Yoneda, K., Tamaki, T., Ota, Y., & Kurazume, R. (2003). Design of bipedal robot with reduced degrees of freedom. *Journal of the Robotics Society of Japan*, *21*(5), 546-553.

Zhang, Q., & Li, H. (2007). Moea/d: A multiobjective evolutionary algorithm based on decomposition. *IEEE Transactions on Evolutionary Computation*, *11*(6), 712-731.

Algorithm 1: Pseudo-code of the proposed MOSPDE algorithm.

Set $G = 1$, $Count_{reset_\varphi} = 1$, $Count_{repeat_\varphi} = 0$, $\epsilon_\varphi = 1E-7$.
Create three random initial parent subpopulations $\mathbf{X}_{G_\varphi}\ \forall\ \varphi = 1, ..., 3$.
Create three empty external populations $EM_\varphi = \varnothing\ \forall\ \varphi = 1, ..., 3$.
Create three empty child subpopulations $\mathbf{U}_{G_{\varphi=\varnothing}}\ \forall\ \varphi = 1, ..., 3$.
Evaluate $\mathbf{J}(\vec{x}^i_{G_\varphi})$, $\mathbf{g}(\vec{x}^i_{G_\varphi})$, $\mathbf{h}(\vec{x}^i_{G_\varphi})\ \forall\ i = 1, ..., NP \wedge \forall\ \varphi = 1, 2, 3$.
while *($G \leq DEF * G_{Max}$)* **do**
    for $i = 1$ *to* NP **do**
        Select randomly $\left\{r_{1_\varphi} \neq r_{2_\varphi} \neq r_{3_\varphi} \neq i\right\} \in \vec{x}^i_{G_\varphi}\ \forall\ i = 1, ..., NP \wedge \forall\ \varphi = 1, 2, 3$.
        j_{rand} =randint$(1, D)$.
        for $j = 1$ *to* D **do**
            Generate the child individual $\vec{u}_{G+1_\varphi}$ of each subpopulation by applying the corresponding the mutation and crossover process in (21).
        Evaluate $\mathbf{J}(\vec{u}^i_{G+1_\varphi})$, $\mathbf{g}(\vec{u}^i_{G+1_\varphi})$, $\mathbf{h}(\vec{u}^i_{G+1_\varphi})\ \forall\ \varphi = 1, 2, 3$.
        Choose between $\vec{u}^i_{G+1_\varphi}$ and $\vec{x}^i_{G+1_\varphi}$ the individual per each subpopulation which pass to the next generation based on the proposed selection process given in Algorithm 2 and store in $\vec{x}_{G+1_\varphi}\ \forall\ \varphi = 1, ..., 3$.
    Filtered process to accept $\vec{x}_{G+1_\varphi}\ \forall\ \varphi = 1, ..., 3$ into the corresponding memory EM_φ.
    Eliminate individual excesses in the memories by using the sudden extinction mechanism given in Algorithm 5.
    Intercommunicate the subpopulations $\varphi = 2$ and $\varphi = 3$ by using the share and reset strategy in Algorithm 3 .
    $G = G + 1$.
Collect all external memories $EM_\varphi\ \forall\ 1, 2, 3$ into the central external memory CEM by using a filter process.
Only $\mathbf{X}_{G_1}$ continue in the next evolution process, i.e., only the population $\varphi = 1$.
while *($G \leq G_{Max}$)* **do**
    Ascending sort of CEM with respect to a performance function.
    for $i = 1$ *to* NP **do**
        Select randomly the base vector index $\{r_{1_1} \neq i\} \in CEM$ in the less crowded region.
        Chose the corresponding two random difference vector indexes $\{r_{2_1} \neq r_{3_1} \neq i \neq r_{1_1}\} \in \Xi$ of CEM where the neighborhood Ξ is based on Algorithm 4.
        j_{rand} =randint$(1, D)$.
        for $j = 1$ *to* D **do**
            Generate the child individual $\vec{u}_{G+1_1}$ by applying the corresponding the mutation and crossover process in (21) .
        Evaluate $\mathbf{J}(\vec{u}^i_{G+1_1})$, $\mathbf{g}(\vec{u}^i_{G+1_1})$, $\mathbf{h}(\vec{u}^i_{G+1_1})$.
        Choose between $\vec{u}^i_{G+1_1}$ and $\vec{x}^{r_{1_1}}_{G+1_1}$ the individual of the population which pass to the next generation based on the proposed selection process given in Algorithm 2 and store in $\vec{x}_{G+1_1}$.
    Filtered process to accept $\vec{x}_{G+1_1}$ into the central external memory CEM.
    Eliminate the individual excesses in the CEM by using the sudden extinction mechanism given in Algorithm 5 .
    $G = G + 1$.
The designer will select the appropriate trade-off in CEM.

Algorithm 2: Pseudo-code of the proposed selection process between the $i-th$ parent $\vec{x}^{i}_{G_\varphi}$ and child $\vec{v}^{i}_{G_\varphi}$ of the $\varphi-th$ subpopulations.

```
if both individuals are feasible then
    if one individual dominates the other then
        Select the non-dominated individual.
    else
        if G ≤ (DEF * G_Max) then
            The individual is selected according to its corresponding subpopulation φ.
            switch φ do
                case 1 do
                    Select randomly the individual.
                case 2 do
                    Select the individual with the best performance in J_1.
                case 3 do
                    Select the individual with the best performance in J_2.
        else
            Select the child individual.
else
    if one of the two individuals are feasible then
        Select the feasible individual.
    else
        if both are infeasible and one presents fewer total amount of constraint violations then
            Chose the individual with the smaller overall constraint violation.
        else
            This is the case when the same constraint violation number results, then the individual which
            presents less o equal constraint distance (i.e., less amount of Σ_1^{n_g} max{g_i, 0}) is preferred.
```

Algorithm 3: Share and reset strategy for the subpopulation $\varphi = 2$ and $\varphi = 3$.

```
Sort in ascending order the φ − th subpopulation with respect to J_{φ−1}.
Store the first (best) and last (worse) individual of the sorted subpopulation in I⃗_{best_φ,G} and I⃗_{worse_φ,G},
  respectively.
if J(I⃗_{best_φ,G−1}) < J(I⃗_{best_φ,G}) then
    Count_{repeat_φ} = 0.
else
    if J(I⃗_{best_φ,G−1}) == J(I⃗_{best_φ,G}) then
        Count_{repeat_φ} = Count_{repeat_φ} + 1.
if |J(I⃗_{worse_φ,G}) − J(I⃗_{best_φ,G})| < ε_φ & X_{G_φ} ∈ Ω̂ then
    Randomly initialize NP − 2 individuals of the φ − th subpopulation.
    Include the best individuals of both subpopulations (I⃗_{best_2} and I⃗_{best_3}).
    ε_φ = ε_φ/10.
    Count_{repeat_φ} = 0.
if Count_{repeat_φ} = 5000 then
    Randomly initialize NP − 2 individuals of the φ − th subpopulation.
    Include the best individuals of both subpopulations (I⃗_{best_2} and I⃗_{best_3}).
    Count_{repeat_φ} = 0.
if G == G_reset * Count_{reset_φ} then
    Randomly initialize NP − 2 individuals of the φ − th subpopulation.
    Include the best individuals of both subpopulations (I⃗_{best_2} and I⃗_{best_3}).
    Count_{repeat_φ} = 0.
    Count_{reset_φ} = Count_{reset_φ} + 1.
```

Algorithm 4: Setting of the neighborhood radius Ξ of the base vector $\vec{x}_{G_1}^{r_{1_1}}$. The central external memory CEM must be previously sorted with respect to a performance function.

Compute the number of individuals n_Ξ corresponding to the neighborhood Ξ in CEM, i.e., $n_\Xi = \Xi * n_{CEM}/100$.
if $r_{1_1} \leq n_\Xi/2$ **then**
    Chose Ξ as the first n_Ξ non-dominated solution in the sorted memory CEM.
else
    if $r_{1_1} \geq n_{CEM} - n_\Xi/2$ **then**
        Set Ξ as the last n_Ξ non-dominated solutions in the sorted memory CEM.
    else
        Chose Ξ as the corresponding non-dominated individuals of the sorted memory in the interval (neighborhood indexes) $[r_{1_1} - n_\Xi/2, r_{1_1} + n_\Xi/2]$.

Algorithm 5: Sudden extinction mechanism.

if *memory is out of its limits* **then**
    Count and store in ξ the number of exceeded non-dominated solutions in the memory.
    Ascending sorting of the memory based on the crowding distance.
    Eliminate the first ξ solutions in the sorted memory.

Table 3.: Parameters of the chosen search approaches of the multi-objective optimizers

Pareto-based optimizer	Parameters			
MOSPDE	$F \in [0.3, 0.9]$	$CR = 0.85$	$DEF = 0.54$	$G_{reset} = 25000$
	$EM_\varphi = 100$			
MODE	$F \in [0.3, 0.9]$	$CR = 0.85$		
CR-MODE	$F \in [0.3, 0.9]$	$CR = 0.85$	$NS = 0.54$	
MOEEDE	$F \in [0.3, 0.9]$	$CR = 0.85$	$EEF = 0.54$	$BP2 = 2NP$
	$n_{MaxInd} = 40$	$n_{row} = 10$	$n_{col} = 10$	
NSGA-II	$pm = 0.083$	$pc = 0.9$	$\eta_c = 20$	$\eta_m = 100$
MOPSO	$W = 0.4$	R_1, $R_2 \in [0, 1]$		
Decomposition search based optimizer	Parameters			
MOEA/D-DE	$F = 0.5$	$CR = 0.5$	$T = 6$	
Metric-driven search based optimizer	Parameters			
SMS-EMOA	$pm = 0.083$	$pc = 1$	$\eta_c = 20$	$\eta_m = 100$

Table 4.: Descriptive statistic summary of the performance metric behavior per each multi-objective optimizer. The best results obtained from the sample are remarked in boldface.

Algorithm	$mean(HV)$	$\sigma(HV)$	$mean(ONVG)$	$\sigma(ONVG)$	CT
CR-MODE	0.999559	0.000116	163.633333	48.961268	10.186044
MODE	0.998538	0.000128	26.766667	4.924837	1.736137
MOEEDE	0.999791	0.000113	**294.000000**	32.486602	19.900577
MOPSO	0.958602	0.030241	285.800000	47.673748	58.019627
NSGA-II	0.999511	0.000512	100.000000	**0.000000**	3.501527
MOEA/D-DE	0.999511	0.000198	200.000000	**0.000000**	**0.755872**
SMS-EMOA	0.999648	0.000076	200.000000	**0.000000**	18.177795
MOSPDE	**0.999976**	**0.000018**	281.133333	23.885840	20.028367

Table 5.: Rank average from all runs achieved by the Friedman test in the performance metrics per each multi-objective optimizer. The computed statistics and related p-value are also shown. The algorithms where the rank average presents the best results are remarked in boldface.

Algorithms	HV Ranks	ONVG Ranks
CR-MODE	4.9	5.467
MODE	6.967	8
MOEA/D-DE	4.8	4.667
MOEEDE	2.533	**1.667**
MOPSO	8	2
MOSPDE	**1**	2.633
NSGA-II	3.967	6.9
SMS-EMOA	3.833	4.667
Statistic	177.2	188.5
p-value	7.7658E-35	3.0782E-37

Table 6.: Adjusted p-values for HV tests for multiple comparisons among all methods. MOSPDE wins six times. MOEEDE wins four times. CR-MODE, NSGA-II, MOEA/D-DE, and SMS-EMOA win two times. MODE and MOPSO do not win.

Hypotesis[1]	Unajusted p[1]	Holm[1]	Shaffer[1]	z
CR-MODE vs MODE	**1.0843E-03**	**1.1927E-02**	**1.1927E-02**	-3.268
CR-MODE vs MOEA/D-DE	8.7437E-01	1	1	0.1581
CR-MODE vs **MOEEDE**	**1.8254E-04**	**2.5556E-03**	**2.3730E-03**	3.742
CR-MODE vs MOPSO	**9.5093E-07**	**1.7117E-05**	**1.5215E-05**	-4.902
CR-MODE vs **MOSPDE**	**6.9844E-10**	**1.5366E-08**	**1.4667E-08**	6.166
CR-MODE vs NSGA-II	1.4002E-01	6.4183E-01	6.4183E-01	1.476
CR-MODE vs SMS-EMOA	**9.1690E-02** **	6.4183E-01	6.4183E-01	1.687
MODE vs **MOEA/D-DE**	**6.1299E-04**	**7.3559E-03**	**7.3559E-03**	3.426
MODE vs **MOEEDE**	**2.3881E-12**	**5.9702E-11**	**5.0150E-11**	7.01
MODE vs MOPSO	1.0229E-01	6.4183E-01	6.4183E-01	-1.634
MODE vs **MOSPDE**	**0**	**0**	**0**	9.434
MODE vs **NSGA-II**	**2.1014E-06**	**3.5724E-05**	**3.3623E-05**	4.743
MODE vs **SMS-EMOA**	**7.2615E-07**	**1.3797E-05**	**1.1618E-05**	4.954
MOEA/D-DE vs **MOEEDE**	**3.3848E-04**	**4.4003E-03**	**4.4003E-03**	3.584
MOEA/D-DE vs MOPSO	**4.2004E-07**	**8.4008E-06**	**6.7206E-06**	-5.06
MOEA/D-DE vs **MOSPDE**	**1.8745E-09**	**3.9364E-08**	**3.9364E-08**	6.008
MOEA/D-DE vs NSGA-II	1.8763E-01	6.4183E-01	6.4183E-01	1.318
MOEA/D-DE vs SMS-EMOA	1.2640E-01	6.4183E-01	6.4183E-01	1.528
MOEEDE vs MOPSO	**0**	**0**	**0**	-8.644
MOEEDE vs MOSPDE	**1.5333E-02**	1.5333E-01	1.5333E-01	2.424
MOEEDE vs NSGA-II	**2.3433E-02**	2.1090E-01	2.1090E-01	-2.266
MOEEDE vs SMS-EMOA	**3.9833E-02**	3.1866E-01	3.1866E-01	-2.055
MOPSO vs **MOSPDE**	**0**	**0**	**0**	11.07
MOPSO vs **NSGA-II**	**1.8028E-10**	**4.1465E-09**	**3.7860E-09**	6.377
MOPSO vs **SMS-EMOA**	**4.4555E-11**	**1.0693E-09**	**9.3566E-10**	6.588
MOSPDE vs NSGA-II	**2.7226E-06**	**4.3561E-05**	**4.3561E-05**	-4.691
MOSPDE vs SMS-EMOA	**7.4680E-06**	**1.1202E-04**	**1.1202E-04**	-4.48
NSGA-II vs SMS-EMOA	8.3303E-01	1	1	0.2108

[1] Boldface and boldface with asterisks indicate the winner between the comparison with 5% and 10% significance level, respectively. Without Boldface means that there is no compelling evidence between samples to confirm which algorithm is better, indicating that the differences between such algorithms are due to chance.

Table 7.: Adjusted p-values for ONVG tests for multiple comparisons among all methods. MOEEDE, MOSPDE and MOPSO win five times. MOEA/D-DE and SMS-EMOA win two times. CR-MODE wins one time. NSGA-II and MODE do not win.

Hypotesis[1]	Unajusted p[1]		Holm[1]	Shaffer[1]	z
CR-MODE vs MODE	**6.1873E-05**		**8.0435E-04**	**8.0435E-04**	-4.006
CR-MODE vs MOEA/D-DE	2.0590E-01		1	1	1.265
CR-MODE vs **MOEEDE**	**1.8745E-09**		**4.1238E-08**	**3.9364E-08**	6.008
CR-MODE vs **MOPSO**	**4.2226E-08**		**8.8674E-07**	**8.8674E-07**	5.481
CR-MODE vs **MOSPDE**	**7.4680E-06**		**1.1949E-04**	**1.1949E-04**	4.48
CR-MODE vs NSGA-II	**2.3433E-02**		1.8746E-01	1.8746E-01	-2.266
CR-MODE vs SMS-EMOA	2.0590E-01		1	1	1.265
MODE vs **MOEA/D-DE**	**1.3608E-07**		**2.7216E-06**	**2.1773E-06**	5.27
MODE vs **MOEEDE**	**0**		**0**	**0**	10.01
MODE vs **MOPSO**	**0**		**0**	**0**	9.487
MODE vs **MOSPDE**	**0**		**0**	**0**	8.485
MODE vs NSGA-II	**8.1990E-02**	**	5.7393E-01	5.7393E-01	1.739
MODE vs **SMS-EMOA**	**1.3608E-07**		**2.7216E-06**	**2.1773E-06**	5.27
MOEA/D-DE vs **MOEEDE**	**2.1014E-06**		**3.7826E-05**	**3.3623E-05**	4.743
MOEA/D-DE vs **MOPSO**	**2.4827E-05**		**3.7240E-04**	**3.7240E-04**	4.216
MOEA/D-DE vs **MOSPDE**	**1.3045E-03**		**1.3045E-02**	**1.3045E-02**	3.215
MOEA/D-DE vs NSGA-II	**4.1366E-04**		**4.9640E-03**	**4.9640E-03**	-3.531
MOEA/D-DE vs SMS-EMOA	1		1	1	0
MOEEDE vs MOPSO	5.9816E-01		1	1	-0.527
MOEEDE vs MOSPDE	1.2640E-01		7.5843E-01	7.5843E-01	-1.528
MOEEDE vs NSGA-II	**2.2204E-16**		**5.5511E-15**	**4.6629E-15**	-8.275
MOEEDE vs SMS-EMOA	**2.1014E-06**		**3.7826E-05**	**3.3623E-05**	-4.743
MOPSO vs MOSPDE	3.1664E-01		1	1	-1.001
MOPSO vs NSGA-II	**9.3259E-15**		**2.2382E-13**	**1.9584E-13**	-7.748
MOPSO vs SMS-EMOA	**2.4827E-05**		**3.7240E-04**	**3.7240E-04**	-4.216
MOSPDE vs NSGA-II	**1.5178E-11**		**3.4909E-10**	**3.1873E-10**	-6.746
MOSPDE vs SMS-EMOA	**1.3045E-03**		**1.3045E-02**	**1.3045E-02**	-3.215
NSGA-II vs **SMS-EMOA**	**4.1366E-04**		**4.9640E-03**	**4.9640E-03**	3.531

[1] Boldface and boldface with asterisks indicate the winner between the comparison with 5% and 10% significance level, respectively. Without Boldface means that there is no compelling evidence between samples to confirm which algorithm is better, indicating that the differences between such algorithms are due to chance.

Table 8.: Performance metrics of the Filtered Pareto front of the multi-objective optimizers. The best performance is remarked in boldface.

Comparison	*HV*	ONVG
CR-MODE	0.999651	235.000000
MODE	0.996682	47.000000
MOEEDE	0.999853	392.000000
MOPSO	0.989319	303.000000
NSGA-II	0.999627	203.000000
MOEA/D-DE	0.999408	245.000000
SMS-EMOA	0.999752	347.000000
MOSPDE	**0.999977**	**571.000000**

Table 9.: Two-set-coverage metric (C-metric) of the filtered Pareto front between algorithms. The best performance is remarked in boldface. MOEA/D-DE wins seven times. MOSPDE wins six times. MOEEDE wins five times. CR-MODE wins four times. NSGA-II wins three times. SMS-EMOA wins two times. MODE wins one time. MOPSO does not win.

Algorithm	C-metric
CR-MODE vs MODE	1.000000
MODE vs **CR-MODE**	0.000000
CR-MODE vs **MOEEDE**	0.000000
MOEEDE vs CR-MODE	1.000000
CR-MODE vs MOPSO	1.000000
MOPSO vs **CR-MODE**	0.000000
CR-MODE vs NSGA-II	0.778325
NSGA-II vs **CR-MODE**	0.489362
CR-MODE vs **MOEA/D-DE**	0.004082
MOEA/D-DE vs CR-MODE	0.804255
CR-MODE vs SMS-EMOA	0.919308
SMS-EMOA vs **CR-MODE**	0.000000
CR-MODE vs **MOSPDE**	0.126095
MOSPDE vs CR-MODE	0.668085
MODE vs **MOEEDE**	0.000000
MOEEDE vs MODE	1.000000
MODE vs MOPSO	1.000000
MOPSO vs **MODE**	0.000000
MODE vs **NSGA-II**	0.000000
NSGA-II vs MODE	1.000000
MODE vs **MOEA/D-DE**	0.000000
MOEA/D-DE vs MODE	1.000000
MODE vs **SMS-EMOA**	0.000000
SMS-EMOA vs MODE	1.000000
MODE vs **MOSPDE**	0.000000
MOSPDE vs MODE	1.000000
MOEEDE vs MOPSO	1.000000
MOPSO vs **MOEEDE**	0.000000
MOEEDE vs NSGA-II	0.891626
NSGA-II vs **MOEEDE**	0.035714
MOEEDE vs **MOEA/D-DE**	0.134694
MOEA/D-DE vs MOEEDE	0.165816
MOEEDE vs SMS-EMOA	1.000000
SMS-EMOA vs **MOEEDE**	0.000000
MOEEDE vs **MOSPDE**	0.304729
MOSPDE vs MOEEDE	0.433673
MOPSO vs **NSGA-II**	0.000000
NSGA-II vs MOPSO	1.000000
MOPSO vs **MOEA/D-DE**	0.000000
MOEA/D-DE vs MOPSO	1.000000
MOPSO vs **SMS-EMOA**	0.000000
SMS-EMOA vs MOPSO	1.000000
MOPSO vs **MOSPDE**	0.000000
MOSPDE vs MOPSO	1.000000
NSGA-II vs **MOEA/D-DE**	0.057143
MOEA/D-DE vs NSGA-II	0.586207
NSGA-II vs SMS-EMOA	0.847262
SMS-EMOA vs **NSGA-II**	0.270936
NSGA-II vs **MOSPDE**	0.208406
MOSPDE vs NSGA-II	0.802956
MOEA/D-DE vs SMS-EMOA	0.841499
SMS-EMOA vs **MOEA/D-DE**	0.000000
MOEA/D-DE vs MOSPDE	0.225919
MOSPDE vs **MOEA/D-DE**	0.016327
SMS-EMOA vs **MOSPDE**	0.005254
MOSPDE vs SMS-EMOA	0.991354

Table 10.: Design variables of the selected trade-offs obtained by MOSPDE.

$\vec{x}^{t*}_{MOSPDE}$									
$f_1^*(\vec{x}^*)$	$f_2^*(\vec{x}^*)$	x_1^*/l_1	x_2^*/l_2	x_3^*/l_3	x_4^*/l_4	x_5^*/l_5	x_6^*/l_6	x_7^*/l_7	x_8^*/l_8
4.189E−5	3.443	0.0976	0.0573	0.0865	0.1267	0.1454	0.0212	0.1495	0.1064
x_9^*/l_9	x_{10}^*/l_{11}	x_{11}^*/l_{12}	x_{12}^*/l_{14}	x_{13}^*/θ_1	x_{14}^*/θ_5	$x_{15}^*/\hat{\theta}_1$	$x_{16}^*/\hat{\theta}_5$	$x_{17}^*/\hat{\theta}_7$	$x_{18}^*/\bar{x}_{ini}$
0.0795	0.1487	0.1101	0.1367	2.5658	4.0465	0.1215	2.4898	1.1701	−0.0330
x_{19}^*/m_{4b_1}	x_{20}^*/m_{4b_2}	x_{21}^*/m_{5b}	x_{22}^*/θ_2^1	x_{23}^*/θ_2^2	x_{24}^*/θ_2^3	x_{25}^*/θ_2^4	x_{26}^*/θ_2^5	x_{27}^*/θ_2^6	x_{28}^*/θ_2^7
1	1	1	2.8247	2.8552	2.8875	2.9208	2.9573	3.0011	3.0574
x_{29}^*/θ_2^8	x_{30}^*/θ_2^9	x_{31}^*/θ_2^{10}	x_{32}^*/θ_2^{11}	x_{33}^*/θ_2^{12}	x_{34}^*/θ_2^{13}	x_{35}^*/θ_2^{14}	x_{36}^*/θ_2^{15}	x_{37}^*/θ_2^{16}	x_{38}^*/θ_2^{17}
3.1219	3.1652	4.2999	4.6027	5.2046	5.8771	0.2800	1.5680	2.3777	2.6990
x_{39}^*/θ_2^{18}	x_{40}^*/θ_2^{19}	x_{41}^*/θ_2^{20}							
2.7330	2.7658	2.7957							
$\vec{x}^{c*}_{MOSPDE}$									
$f_1^*(\vec{x}^*)$	$f_2^*(\vec{x}^*)$	x_1^*/l_1	x_2^*/l_2	x_3^*/l_3	x_4^*/l_4	x_5^*/l_5	x_6^*/l_6	x_7^*/l_7	x_8^*/l_8
4.869E−5	2.935	0.0990	0.0571	0.0863	0.1266	0.1412	0.0214	0.1509	0.1062
x_9^*/l_9	x_{10}^*/l_{11}	x_{11}^*/l_{12}	x_{12}^*/l_{14}	x_{13}^*/θ_1	x_{14}^*/θ_5	$x_{15}^*/\hat{\theta}_1$	$x_{16}^*/\hat{\theta}_5$	$x_{17}^*/\hat{\theta}_7$	$x_{18}^*/\bar{x}_{ini}$
0.0787	0.1500	0.0983	0.1353	2.5766	4.0534	0.1433	2.4931	1.1727	−0.0320
x_{19}^*/m_{4b_1}	x_{20}^*/m_{4b_2}	x_{21}^*/m_{5b}	x_{22}^*/θ_2^1	x_{23}^*/θ_2^2	x_{24}^*/θ_2^3	x_{25}^*/θ_2^4	x_{26}^*/θ_2^5	x_{27}^*/θ_2^6	x_{28}^*/θ_2^7
1	1	1	2.8242	2.8548	2.8915	2.9255	2.9617	3.0072	3.0607
x_{29}^*/θ_2^8	x_{30}^*/θ_2^9	x_{31}^*/θ_2^{10}	x_{32}^*/θ_2^{11}	x_{33}^*/θ_2^{12}	x_{34}^*/θ_2^{13}	x_{35}^*/θ_2^{14}	x_{36}^*/θ_2^{15}	x_{37}^*/θ_2^{16}	x_{38}^*/θ_2^{17}
3.1198	3.1644	4.3320	4.6072	5.1848	5.8338	0.1790	1.6065	2.3772	2.6812
x_{39}^*/θ_2^{18}	x_{40}^*/θ_2^{19}	x_{41}^*/θ_2^{20}							
2.7206	2.7588	2.7926							
$\vec{x}^{*EXT}_{MOSPDE}$									
$f_1^*(\vec{x}^*)$	$f_2^*(\vec{x}^*)$	x_1^*/l_1	x_2^*/l_2	x_3^*/l_3	x_4^*/l_4	x_5^*/l_5	x_6^*/l_6	x_7^*/l_7	x_8^*/l_8
4.1E−6	9.031	0.0846	0.0295	0.1381	0.1831	0.0273	0.0075	0.1456	0.1516
x_9^*/l_9	x_{10}^*/l_{11}	x_{11}^*/l_{12}	x_{12}^*/l_{14}	x_{13}^*/θ_1	x_{14}^*/θ_5	$x_{15}^*/\hat{\theta}_1$	$x_{16}^*/\hat{\theta}_5$	$x_{17}^*/\hat{\theta}_7$	$x_{18}^*/\bar{x}_{ini}$
0.1315	0.1305	0.1458	0.1556	5.3328	2.9470	1.5299	1.3158	1.8502	−0.0763
x_{19}^*/m_{4b_1}	x_{20}^*/m_{4b_2}	x_{21}^*/m_{5b}	x_{22}^*/θ_2^1	x_{23}^*/θ_2^2	x_{24}^*/θ_2^3	x_{25}^*/θ_2^4	x_{26}^*/θ_2^5	x_{27}^*/θ_2^6	x_{28}^*/θ_2^7
1	1	1	2.7728	2.9329	3.0918	3.2428	3.3968	3.5612	3.7434
x_{29}^*/θ_2^8	x_{30}^*/θ_2^9	x_{31}^*/θ_2^{10}	x_{32}^*/θ_2^{11}	x_{33}^*/θ_2^{12}	x_{34}^*/θ_2^{13}	x_{35}^*/θ_2^{14}	x_{36}^*/θ_2^{15}	x_{37}^*/θ_2^{16}	x_{38}^*/θ_2^{17}
3.9190	4.0205	5.4428	5.5418	5.7610	6.0413	0.0770	0.7298	1.2148	2.0198
x_{39}^*/θ_2^{18}	x_{40}^*/θ_2^{19}	x_{41}^*/θ_2^{20}							
2.2425	2.4406	2.6124							